AD

AD 644889

TECHNICAL REPORT ECOM – 01788 – F

TRANSIENT RADIATION DAMAGE IN SEMICONDUCTOR MATERIALS

CLEARINGHOUSE
FOR FEDERAL SCIENTIFIC AND TECHNICAL INFORMATION
Hardcopy | Microfiche
$3.00 | $.65 | 89 pp | as
1 ARCHIVE COPY

FINAL REPORT

BY

J.C. CORELLI – A.R. FREDERICKSON
J.W. WESTHEAD

DECEMBER 1966

"This Research is Sponsored by the Defense Atomic Support Agency Under NWER Subtask 16.0091."

ECOM

UNITED STATES ARMY ELECTRONICS COMMAND
FORT MONMOUTH, NEW JERSEY

DDC
JAN 12 1967

CONTRACT DA28-043 AMC-01788(E)

RENSSELAER POLYTECHNIC INSTITUTE
TROY, NEW YORK

DISTRIBUTION OF THIS DOCUMENT IS UNLIMITED

Technical Report ECOM-01788-F December 1966

TRANSIENT RADIATION
DAMAGE IN SEMICONDUCTOR MATERIALS

Final Report

1 October 1965 to 30 September 1966

Report No. 4

Contract No. DA 28-043 AMC-01788(E)
AMC Code 5900 21 830 44 00 (DASA)

This research is sponsored by the
Defense Atomic Support Agency under NWER Subtask 16.0091.

Prepared by:
Dr. John C. Corelli
Mr. A. Robb Frederickson

Rensselaer Polytechnic Institute
Troy, New York

for

U. S. Army Electronics Command, Fort Monmouth, N. J.

DISTRIBUTION OF THIS DOCUMENT IS UNLIMITED

I. Abstract

The transient behavior of the resistivity and Hall effect voltage in 1 to 100 ohm-cm n- and p-type silicon has been studied both during and after exposing the sample to short bursts (0.01 to 4.5 microseconds) of 48 MeV electrons. The buildup of excess electrons produced by ionization during the time the electron pulse is irradiating the sample appears to be dependent on the normal excess carrier decay rate. The injection levels induced by the bombarding electrons are high ($\frac{\Delta n}{n} > 10^{-1}$) and in most cases the excess carrier lifetimes exhibit an increase with higher injection level. The number of excess carriers generated as a function of electron beam intensity can be calculated to within a factor of 2 from a knowledge of the ionization energy loss, the energy to form an electron-ion pair, and the total integrated electron flux. The temperature dependence of induced conductivity as a function of injection is consistent with that predicted by theory. The transient Hall voltage response of 100 ohm-cm p-type silicon for high injection levels can be approximately reproduced by calculation assuming mixed hole-electron conduction and equal hole and electron decay times by a single time dependent exponential. A simple model is given which describes fast annealing in 45-50 MeV electron-irradiated silicon. The single dominant "radiation damage" process which occurs in all cases is the production of excess carriers from ionization of lattice atoms and their subsequent decay by recombination. Atomic displacement effects as manifested by the electronic transport properties appear to be very small and insignificant.

II. Table of Contents

Page

I. Abstract i

II. Table of Contents ii

III. Introduction 1

IV. Experimental Methods 2

V. Results and Discussion 3

Table I 4

VI. Conclusions 22

VII. Recommendations and Suggestions for Future Experiments 25

References 29

Figure 1 - Block diagram of overall electronic system and current pulser schematic circuit diagram showing how pulsed sample current system operates 31

Figure 2 - Excess carrier generation vs. total integrated electron beam flux (296°K) for SC-28 32

Figure 3 - Excess carrier generation vs. total integrated electron beam flux (122°K) for SC-28 33

Figure 4 - Excess carrier generation vs. total integrated electron beam flux (296°K) for SC-30 34

Figure 5 - Excess carrier lifetime vs. total flux for SC-30 35

Figure 6 - Excess carrier lifetime vs. total flux (298°K) for SC-23 36

Figure 7 - Excess carrier lifetime vs. total flux for SC-22 37

Figure 8 - Excess carrier lifetime vs. total flux for SC-16 38

Table of Contents Contd.

Page

Figure 9 - Transient Hall and resistivity voltage resulting from bombardment of 10 ohm-cm n-type silicon (sample SC-24)............ 39

Figure 10 - Dependence of lifetime on injection as measured by injected excess carrier concentration, Δn (electrons/cm^3), or fractional resistivity change $\frac{\Delta\rho}{\rho}$ 40

Figure 11 - Hall voltage response of 100 ohm-cm p-type silicon (sample SC-31) after exposure to 48 MeV electron pulses of three different total integrated pulses.. 41

Figure 12 - Comparison of measured and calculated time dependence of Hall voltage for 100 ohm-cm p-type silicon (sample SC-31) irradiated at 300°K by 48 MeV electrons.. 42

Figure 13 - Excess carrier lifetime vs. total integrated flux (296°K) for SC-31........ 43

Figure 14 - Dependence of lifetime on injection as measured by excess hole concentration Δp (holes/cm^3) or fractional resistivity change $\frac{\Delta\rho}{\rho}$ 44

Figure 15 - Dependence of lifetime on injection as measured by excess hole concentrations Δp (holes/cm^3) or fractional resistivity change $\frac{\Delta\rho}{\rho}$ 45

Figure 16 - Calculated fraction of damage remaining in n- and p-type silicon vs. time after irradiation by 48 MeV electron beam pulses.................................. 46

Appendix (Report entitled "Transient Ionization Effects in Silicon Induced by 48 MeV Electron Pulses")... 47

III. Introduction

This Final Report gives the presentation and summary of all research conducted in the time interval 1 October 1965 through 1 October 1966 on the RPI Transient Radiation Damage in Semiconductor Materials program. The primary goal and purpose of the program was to investigate the mechanisms which are basic and important to an understanding of the general problem of the effects in silicon irradiated with a pulse of radiation. The radiation used in this investigation was electrons from the Rensselaer 5-80 MeV pulsed electron Linac. At the outset of the program it was expected that damaging effects arising from 50 MeV electrons would not be as pronounced as those which arise from fast neutron pulsed irradiation but on the other hand the electron effects would be more pronounced than those effects from pulsed low energy ($\lesssim 2$ MeV) gamma rays. Of course in the comparison we are assuming equal total integrated fluxes of all the types of radiation just mentioned.

The main emphasis of the program of research which we have followed was to study the transient effects of 50 MeV electron bursts on the electrical properties of silicon. The properties measured were resistivity and Hall effect voltage and the carrier recombination lifetime; the measurements were made both during and after the electron beam pulse. The research work in this program was intended to relate and provide some understanding as a contribution to the more widespread

effort on Transient Radiation Effects on Electronics (TREE), in particular to provide a basis for explaining what occurs in semiconductor devices fabricated from silicon.

In order to obtain a maximum amount of information regarding the behavior of silicon in a pulsed electron environment our irradiation experiments were perfromed on silicon material doped with a fairly large range of impurity concentration, $\sim 10^{13}$ to 10^{16} atoms/cm^3. The dopants were boron, indium and phosphorus, and the single crystals utilized included mostly zone refined (FZ for floating zone) material with $< 10^{16}$ oxygen atoms/cm^3 although some pulled crystals with $> 10^{17}$ oxygen atoms/cm^3 were also studied. Additionally, we also sought to investigate temperature effects on the transient radiation damage process hence we performed some irradiations with the sample temperature maintained in the 100°K to 300°K range.

We have previously reported our results in the form of a paper,[1] a copy of which is included at the end of this report as an appendix, while other portions of our research results have appeared in three earlier quarterly progress reports.[2]

IV. Experimental Methods

A complete description of the experimental methods and techniques used in the irradiation experiments is given in the paper attached at the end of this report as an appendix and we shall not repeat here any discussion appearing in the attached paper. One new experimental technique was attempted which was

not reported on previously and will be discussed here briefly. In order to increase the accuracy of measurement of excess carriers at large injection produced by the higher electron beam intensity pulses a new device was constructed. The device works as follows: within 0.15 μsec after the incident 50 MeV electron beam pulse strikes the sample a large current is passed thru the sample and the resulting resistivity voltage is recorded on an oscilloscope. This large current is adjusted so that the resistivity voltage from the sample will be between 5 and 500 mV; such a voltage is low enough that no carrier sweep-out occurs, yet sufficiently large as to be easily measurable on an oscilloscope. The duration of time in which current flows through the sample is sufficiently short ($\lesssim$ 500 millisec) that the sample is not heated to a higher temperature. The block diagram showing schematically how the sample current pulsing device is used is given in Fig. 1. The device allowed us to irradiate the sample with high total dose in the pulse while preventing the occurrence of voltage saturation described in detail elsewhere.[1] Although the device accomplished what it was intended to do, further development aimed at reducing signal noise would have been necessary, but this was not possible because the research program was to be brought to an orderly conclusion.

V. Results and Discussion

In Table I is given a list of some of the samples which have been studied. The values of resistivity, carrier concentration, and Hall mobility before irradiation are given together with the

TABLE I

Properties of Silicon Samples Before Pulsed Irradiations With 48 MeV Electrons

Sample Type and Code Number		Dopant	Temperature °K	Resistivity ohm-cm	Carrier Concentration cm^{-3}	Hall Mobility cm^2/volt-sec
n-type Si						
SC-33	FZ	Phosphorous	299	17.4	2.1×10^{14}	1720
p-type Si						
SC-34	FZ	Boron	299	0.85	2.2×10^{16}	338
p-type Si						
SC-36	FZ	Boron	229	10.3	1.5×10^{15}	400

FZ indicates sample was cut from floating zone silicon.

sample dopant. The complete set of samples studied in the investigation also includes those listed in the paper attached as an appendix. In the main body of this report we shall not repeat any of the results or discussion which have already been given in the attached paper. However, if the previously given results were analyzed further and allowed additional conclusions and interpretations to be made they will be included here.

A. n-Type Silicon Samples

In both n- and p-type silicon large numbers of excess carriers are produced from the ionization of atomic electrons by energy imparted to them by the bombarding electrons. The beam characteristics of the Linac are such that ionization-induced excess carrier concentrations of $\sim 10^{16}$ - 10^{17} cm^{-3} can be achieved easily. Excess carrier concentrations as are produced by the electron beam lead immediately to high injection level effects on the lifetime and on the damage mechanism. These points will be discussed below in greater detail.

An important effect of high intensity ionizing radiation is to cause the material to become temporarily intrinsic where one has mixed electron and hole conduction; for such a semiconductor we can write the conductivity as

$$\sigma = ne\mu_n + pe\mu_p \qquad (1)$$

where:

n = number of conducting electrons

p = number of conducting holes

e = electron charge

μ_n = conduction electron mobility

μ_p = conduction hole mobility

The ratio of Hall to drift mobility was put equal to unity and we have neglected the temperature dependence of this ratio in all subsequent discussions included in this report. We have made the assumptions that μ_n and μ_p remain constant during the time excess electrons are produced by ionization and decay by recombination processes. This assumption has been proved to be valid* for purposes of our experiment. We further assume that $\Delta n = \Delta p$ i.e., equal numbers of excess electrons and holes are produced by the electron pulse. Using equation 1 and the above assumptions we derive for n- and p-type semiconductors the following expressions for the injection for n and p type respectively

$$\frac{\Delta n}{n_o} = \frac{-\Delta V_\rho}{V_{\rho_o} - \Delta V_\rho} \frac{\mu_n}{\mu_n + \mu_p} \qquad \frac{\Delta p}{p_o} = \frac{-\Delta V_\rho}{V_{\rho_o} - \Delta V_\rho} \frac{\mu_p}{\mu_n + \mu_p} \tag{2}$$

where p_o, n_o, V_{ρ_o} are the steady state pre-irradiation values of hole and electron carrier concentrations and resistivity voltage respectively. The formulas in Eq. 2 above were used to obtain the excess carrier concentration from the measuredvoltage change ΔV_ρ during the irradiation and the quiescent dc value V_{ρ_o}.

The number of excess carriers produced by the electrons in a given pulse was estimated from tables on the ionization energy loss in matter,[3] the energy required to form an electron-ion pair which is 3.5 eV+ for silicon, and a knowledge of the total

---

* Our measurements have shown mobility changes of less than about 10% for the most intense electron beam pulse irradiation of silicon.

\+ For more details see C. Brissolati, A. Fiorentini, and G. Fabri, Phys. Rev., 136A, 1756 (1964).

integrated electron flux. In the calculation we assumed that the electron beam pulse width was small compared to the carrier recombination lifetime. In our estimate we have neglected all effects which arise from temperature. Under these conditions the calculated carrier concentration was given by

$$\Delta n \cong \left(\frac{\#\text{ electrons in 50 MeV pulse}}{\text{cm}^2}\right)\left(\begin{array}{l}\text{energy lost to ionization}\\ \text{per cm in silicon}\end{array}\right)\left(\frac{1}{3.5\text{ eV}}\right)$$

or

$$\Delta n \simeq \frac{2.4 \times 10^6}{\text{cm}} \times \left(\frac{\#\text{ electrons in 50 MeV pulse}}{\text{cm}^2}\right) \quad (3)$$

Comparisons of the measured integrated flux dependence of excess carrier concentration with the calculated values using Eq. 3 above are given in Figs. 2 and 3 for $\approx$1 ohm-cm n-type silicon (sample SC-28) irradiated by 48 MeV electron pulses at 296°K and 122°K respectively. In Fig. 4 the comparison of measured with calculated integrated flux dependence of excess carriers is given for a 10 ohm-cm n-type silicon sample (sample SC-30) irradiated at 296°K by 48 MeV electron pulses. Considering the simplifying assumptions made in the computation the comparison of calculated and measured values shown in Figs. 2, 3 and 4 is considered satisfactory and in fact suggests that for a first approximation to within a factor of 2 one can use this simple calculation to assess ionizing effects of any radiation on semiconductors irrespective of whether the material is in the form of a device or a bulk sample.

The temperature dependence of the excess carrier concentration vs. integrated flux which can be ascertained from the results in Figs. 2 and 3 is very nearly the same as the excess

conductivity vs. integrated flux since the mobility change is small (< 10%) compared to excess carrier concentration increase (factor ∼100). We have compared the temperature dependence of the induced conductivity which was obtained from the results in Figs. 2 and 3 to what is predicted in the theory of Appel.[4] We have found good agreement between the experimental and theoretical temperature dependence of excess conductivity. The theory[4] takes into account only electron-electron and electron-ion scattering processes in deriving an expression for the conductivity. The inclusion of electron-hole scattering effects is expected to be small according to additional theoretical calculations by Appel.[5] In order to make more detailed and meaningful comparisons and to search for the small electron-hole scattering effects additional experiments run at two intermediate temperatures between 122°K and 296°K are required. One would also need to improve the measurement accuracy at high injection levels in order to allow detailed comparisons between experiment and theory to be made. A complete list of samples run is given in Table I in the attached paper and also is supplemented in Table I of this report with samples SC-33, 34 and 36.

In Figs. 5, 6, 7 and 8 we show the dependence of excess carrier recombination lifetime on integrated electron flux in the pulse for three ten ohm-cm n-type silicon samples and one 100 ohm-cm n-type silicon sample. The carrier recombination lifetime τ_n is defined as the time necessary for the number of excess carriers

to decay from $(\Delta n)_o$ to $\frac{\Delta n_o}{e}$; and we measure this time from the oscilloscope traces of transient resistivity voltage V_ρ combined with the formula of Eq. 2. Our results indicate that for n-type silicon of 1 ohm-cm (see Ref. 1) and 10 ohm-cm (see Figs. 5, 6 and 7) the lifetime shows a marked increase with increased injection, whereas this increased lifetime with injection level dependence was not observed in any of the 100 ohm-cm n-type samples (see Fig. 8). Our results on the injection level dependence of lifetime are in general agreement with other workers[6,7] who have found similar effects using different radiations ($\sim$1 MeV electrons and 100-150 keV x-rays) to produce the ionization-induced excess electrons. However, it is possible that the lifetimes measured in our case are due not only to an injection level dependence but also and perhaps of lesser importance to a fast annealing ($\leq$1000 μsec) of a relatively small number* ($\leq 10^{11}$/atoms/cm^3) of displaced atoms produced by a single pulse of 48 MeV electrons. The high sensitivity of carrier lifetime to very low defect concentrations ($\leq 10^{11}$ cm^{-3}) has been shown by Fischer and Corelli[8] for the case of 6 to 88 MeV electron irradiation of n-type germanium; many of the points discussed by them for the case of germanium are also applicable to silicon.

In all silicon samples studied it was found experimentally that the pulsed radiation-induced transient resistivity and Hall effect voltages had the same time dependence irrespective of the

---

* Method used to arrive at this defect concentration will be given below.

sample temperature during irradiation, the electron beam pulse duration or the electron beam peak current. It was relatively simple to follow both Hall and resistivity voltages simultaneously using a dual beam oscilloscope (Tektronix 555). A typical result showing both the Hall and resistivity voltage decay is given in Fig. 9 for a 10 ohm-cm n-type sample (SC-24) irradiated at $300^{o}K$ with a low total dose pulse $\lesssim 10^{7}$ e/cm^{2} and a high total dose pulse $\approx 1.9 \times 10^{10}$ e/cm^{2}. The pulse shapes shown in Fig. 9 are the same and both Hall and resistivity voltage exhibit saturation at high injection levels.* The saturation of voltage has been discussed in detail elsewhere[1] and will not be repeated here.

The final result which we shall present on the n-type silicon samples is given in Fig. 10, where we have plotted the decay constant τ_n as a function of $\frac{\Delta\rho}{\rho}$ for a 17 ohm-cm n-type silicon sample (SC-33) and have shown on the same graph (upper abscissa) the excess carrier concentration corresponding to the fractional percentage change in resistivity. A close examination of the results shown in Fig. 10 shows that to within the experimental error $\pm$ 10% in τ_n and $\frac{\Delta\rho}{\rho}$ the decay constant has a linear dependence on injection. Consequently we can further state that the linear dependence of τ_n on injection (at high injection levels) implies we can view the recombination process using Hall[9] and Shockley and Reed[10] single level recombination theory. For purposes of completeness and benefit of the reader we write down

* Instead of high injection levels one may also state high electron beam intensities since the injection level depends on the beam intensity.

the lifetime-injection level formula for the case of high injection where recombination takes place mainly by one dominant energy level

$$\left(1+\frac{\Delta n}{n}\right)\tau = \tau_o + (\tau_{n_o} + \tau_{p_o})\frac{\Delta n}{n} \qquad (4)$$

τ = decay constant or lifetime

τ_o = small injection lefetime $\Delta n \rightarrow 0$

τ_{p_o} and τ_{n_o} are the hole and electron lifetime when the Fermi level lies near the conduction band or valence band respectively. A more detailed discussion of Eq. 4 for n- and p-type silicon has been given by Baicker[7] while Blakemore[11] has treated the case of injection level dependence in p-type silicon in detail.

B. p-Type Silicon

If p-type silicon having $\sim 10^{14}$ holes/cm^3 is irradiated by a sufficiently intense pulse of ionizing radiation,then excess carriers are produced which have concentrations $\sim$100 times larger than the initial hole concentration. The excess carriers consist of equal numbers of holes and electrons and since electrons have a higher mobility in silicon the conduction of the initially p-type silicon will be converted to n-type for a time duration which depends on the electron-hole recombination. Therefore, under these circumstances one expects and indeed finds that the measured Hall voltage during the "transient" changes sign twice and is experimental verification of the conversion p- to n-type and back to p-type. In order to compare the time dependence of the measured transient Hall voltage following an intense electron beam pulse to calculated values a computer program was written which calculates

the Hall voltage (V_H) response with time from the following equation for mixed conduction by electrons and holes.

$$V_H \propto \frac{p\mu_p^2 - n\mu_n^2}{(p\mu_p + n\mu_n)^2} \qquad (5)$$

where $p = p_o + \Delta p$

$$n = n_o + \Delta n \qquad (6)$$

and μ_n; and μ_p are assumed to remain constant during the production and decay of radiation-induced excess electrons and holes. We assume that both the excess electrons Δn and the excess holes Δp decay by single exponentials given by

$$\Delta p = (\Delta p)_o e^{-t/\tau_p}$$
$$\Delta n = (\Delta n)_o e^{-t/\tau_n} \qquad (7)$$

where $(\Delta n)_o$, $(\Delta p)_o$ are the concentration of excess electrons and holes respectively just after production and before any decay by recombination τ_p and τ_n are the hole and electron decay constants. In the computer program thus far developed we have made the following assumptions regarding the quantities used in Eq. 5 above. The hole (p_o) and electron (n_o) concentrations before the irradiation pulse strikes the sample are obtained from the measured dc values using $R_H = \frac{1}{n_o e}$ or $R_H = \frac{1}{p_o e}$; $(\Delta n)_o = (\Delta p)_o$ i.e., an equal number of electrons and holes are produced by the pulse, and we obtain Δn or Δp from the transient resistivity voltage expressions given in Eq. 2 above. The hole decay constant

τ_p and the electron decay constant τ_n were assumed to be equal for simplicity ($\tau_p = \tau_n = \tau$) in these first calculations. The electron mobility μ_n and the hole mobility μ_p are assumed to remain constant during and immediately following the electron burst.

In Fig. 11 we show the time dependence of the Hall voltage for 100 ohm-cm p-type silicon (SC-31) irradiated with different doses of 48 MeV electrons at 300°K. The pulse labeled 1 is produced by a low electron dose and the concentration of excess electrons produced by the ionization is less than the hole concentration (1.7×10^{14} cm^{-3}), hence the sign of the Hall voltage remains unchanged as is shown in the experimental results of Fig. 11. The pulse labeled 3 in Fig. 11 results from a high electron dose which produces a sufficiently high concentration of excess electrons causing the sample to become temporarily converted to n-type.

A comparison of the measured and calculated time dependence of the Hall effect voltage for a 100 ohm-cm p-type silicon sample irradiated at 300°K with 48 MeV electrons is shown in Fig. 12. The total dose in the pulse $\sim 1.9 \times 10^{10}$ e/cm^2 is sufficiently high to cause the sample conduction type to change from p to n and back to p during a short time interval ≈ 110 μsec. The solid line marked "measured" was obtained from a single pulse. The lifetime of carriers was obtained from the "measured" curve as 14.3 ± 1 μsec by measuring from the peak of the curve to the point where the curve passes through $V_H = 0$. This time is approximately 1.12τ and is calculated using a knowledge of the measured quantities appearing in Eq. 5 in conjunction with Eq. 7. From a

variety of current pulses having various peak heights the injection was measured to be

$$\Delta n = \begin{pmatrix}\text{total integrated electron} \\ \text{flux in one pulse}\end{pmatrix} \times 1.85 \times 10^{-6}\ cm^{-3}$$

Since we know the integrated flux for the "measured" curve we know the initial Δp_o. Assuming single exponential decay of $\Delta n = \Delta p$ with lifetime $\tau = \tau_n = \tau_p = 14.0\ \mu sec$, and starting at $t = 0$ with Δp_o excess holes and electrons, we get the "calculated" curve. Notice that the calculated curve is both "longer" and "higher" than the measured curve. Several possible reasons for the "length" discrepancy are: the 10% experimental error in τ, the 20% error in Δp_o, and a non constant τ during the decay. Possible reasons for the height discrepancy are: $\tau_n \neq \tau_p$, improper assumption for μ_n in p-type material, and some decay mechanism other than exponential. The series of points shown in Fig. 12 represent an experimental plot of V_H for electron pulses of various intensity when we know $\Delta p = \Delta n$. The points were obtained by measuring V_H at $t = 0$ for many differing incident total flux levels since we can safely assume that $\Delta n = \Delta p$ immediately after the electron pulse strikes the sample. We then plot each of these values of the Hall voltage V_H along the time axis so that Δp (points) corresponds in time to the Δp of the calculated curve. i.e.: Δp (calculated) $= \Delta p_o$ (calculated) $e^{-t/\tau}$.

The fact that for the points, where $\Delta p = \Delta n$, we have good agreement with the calculated curve shows that the assumption for μ_n was fairly accurate, and that $\Delta n \neq \Delta p$ during the entire time duration of the decay of excess carriers in silicon.

The injection level (plotted in the form of integrated flux) dependence of decay constant for a 100Ω-cm p-type sample irradiated at 296°K is shown in Fig. 13. Although only a few points are given the results are included since they demonstrate an increase in decay constant with injection level. Another complication in p-type silicon of 100Ω-cm resistivity is that we observe a decrease in decay constant which can be easily detected with successive electron beam pulses. The decrease in decay constant is characteristic of a radiation-induced non-transient effect. In Fig. 14 and Fig. 15 are given additional results on room temperature irradiated silicon where we have plotted the decay constant as a function of fractional resistivity change $\frac{\Delta\rho}{\rho}$, also shown on the upper abscissa are the corresponding excess hole concentrations. The pulsed electron irradiation results given in Figs. 14 and 15 were obtained using 10 ohm-cm p-type silicon (samples SC-34 and SC-35). In Figs. 14 and 15 we again observe the increased decay constant with higher injection which is similar to what Baicker(7) observed in $\approx$1 ohm-cm p-type silicon. We can observe in Figs. 14 and 15 that there is an apparent experimental scatter of points. We have numbered each point given to correspond to the time chronologically when the electron pulse was incident on the sample. With this information given we can again state that permanent radiation damage is the cause of the decrease in decay constant, τ, and is observable as the spread or scatter in the experimental measurements.

C. Description of Fast Annealing ($\lesssim 10^{-3}$ sec) Processes in 48 MeV Electron-Irradiated Silicon

During the past year additional measurements on defects induced in electron-irradiated silicon have made it possible to construct a fairly simple annealing model to arrive at a reasonable understanding of fast annealing in this material. We shall use a simple treatment of annealing in semiconductors, the details of which are given elsewhere.[20] The assumptions of the annealing process will be based on experimental evidence which has been well substantiated. We shall neglect the effect of injection on vacancy reordering in p-type silicon, an effect which was beautifully demonstrated by Gregory[12] in ^{60}Co gamma and by Sander and Gregory[13] in pulsed neutron irradiation of silicon at $\approx 76^{\circ}$K. One essential feature of the results of these workers[12,13] was that in p-type silicon one can change the charge state of the single vacancy defect from neutral (anneals at $\approx 160^{\circ}$K) to negative (anneals at $\approx 60^{\circ}$K) by injecting excess carriers in a sample of silicon irradiated at 76°K. The annealing studies of the vacancy in its various charge states have been reported by Watkins.[14,15] Gregory[12] showed that for 1 ohm-cm p-type silicon injections of $\geq 8 \times 10^{12}$ carriers/cm^3 are sufficient to cause a detectable reduction in damage. An additional assumption we make is that the concentration of displacement clusters from a disordered region produced by recoils from 50 MeV electrons is small and negligible. Kalma, Corelli and Cleland[16] have recently studied disordered regions produced in germanium by 50 MeV electrons and they find one must

expose the sample to very high integrated fluxes in order to observe measurable effects due to disordered regions. Hence it is reasonable to assume that a similar behavior would be expected in silicon and the low electron flux in pulsed electron irradiations would indeed produce only a very low concentration of disordered regions (~200 Å in diameter).

Watkins[14] has shown that the activation energy for vacancy motion (annealing) in p-type silicon is E = 0.33 ± 0.03 eV with a jump frequency of $\nu_o = 2 \times 10^{12}$ sec^{-1}. More recently Watkins[17] has measured the single vacancy in n-type silicon and finds an activation energy of 0.19 ± 0.02 eV with a jump frequency of $\nu_o = 10^{10}$ sec^{-1}. For both n- and p-type silicon the annealing kinetics are monomolecular. It is also significant to point out that detailed annealing studies by Cheng et al.[18] of the silicon divacancy defect using infrared spectroscopy indicate first order annealing kinetics governs the recovery process. Using the above information we can write down an equation which gives the rate of annealing of simple defects produced in electron-irradiated silicon.

$$\frac{dn}{dt} = \nu_o e^{-E/kT} n = Kn \tag{8}$$

or upon integration we have

$$n(t) = n(o)e^{-Kt}$$

where n(t) and n(o) are the defect concentrations at time t and t = o respectively in the annealing process; all other symbols have been defined above. It is important to note that the vacancies which move are able to "attach themselves" to impurities, other

vacancies, dislocations and other defects forming stable complexes. Additionally, we have neglected to take into account the higher order defects, for example the divacancy since its annealing temperature is substantially higher[18] ($\sim 520^{o}K$) than the annealing temperature for single vacancy motion in p-type silicon (~ 160-$180^{o}K$) and in n-type silicon[17] ($\sim 75^{o}K$); consequently we would not expect to see fast annealing of the divacancy.

The carriers removed from the conduction band constitute a reasonable measure of the defect concentration n(t) given above. We make the assumption that each carrier removed, and hence trapped on some defect, represents one defect. Detailed measurements of the carrier removal in 1 to 100 ohm-cm n-type silicon irradiated by 45 MeV electrons at $80^{o}K$ have been reported by Cheng and Corelli.[19] They found that irrespective of doping concentration in the 1 to 100 ohm-cm resistivity range the carrier removal rate was constant $\approx 1\ cm^{-1}$. We now have enough information to quote approximate defect concentrations produced in a typical situation by a single pulse of electrons. For a pulse of electrons having a total integrated flux of 10^{11} e/cm^{2} we would expect to have produced 10^{11} defects/cm^{3} and is equivalent under our assumptions to removing 10^{11} carriers/cm^{3}, which is small in comparison to our typical carrier concentrations 10^{13}-10^{15} cm^{-3}. It would not be possible to detect such a small change in carrier concentration with any presently available oscilloscope - amplifier-camera systems. However, the effects of this small defect concentration on the carrier lifetime decay constant might indeed be detectable during and immediately following the burst of electrons.

It would be of interest to perform an experiment designed to check this point, however, our past experience in transient radiation effects experiments suggest the effect will be difficult to detect because of very low-level signals.

In Fig. 16. we have plotted the fraction of damage remaining n(t)/n(o), as a function of the time after a 50 MeV electron pulse has irradiated the sample. In the calculation we assumed the beam pulse width to be small compared to the lifetime decay constant. The results shown in Fig. 16 apply to n- and p-type silicon irradiated at various temperatures indicated on the figure. The results of the simple (perhaps oversimplified) annealing model applied to 48 MeV electron radiation-induced defects in silicon (see Fig. 16) suggest that the most convenient irradiation temperature to observe fast annealing in p-type silicon is between 180 to 200°K and in n-type silicon is 150°K. At these temperatures one would anticipate observing annealing in times of 100 to 1000 μsec. Another important result which can be "gleaned" from Fig. 16 is that it is not necessary to irradiate below about 100°K in order to observe fast annealing.

D. Discussion of Lifetime Change to Detect Transient Radiation Damage Independent of Injection Level

The carrier recombination lifetime can be a sensitive detector of radiation-induced damage, both transient damage and permanent damage. We seek to explore the possibility of measuring a lifetime change due to damage by say $\approx$50 MeV electrons. The experimental data given earlier (see for example Figs. 5, 6, 7 and

8) shows that lifetime depends on the injection level. For cases where the beam pulse duration is much shorter than the decay lifetime the injection level $\frac{\Delta n}{n_o}$ is directly proportional to the integrated flux; this is not true for cases where ($\tau < 5 \Delta T_B$) the lifetime τ is less than 5 times the duration of the electron beam ΔT_B. Thus we can change the injection level vs. integrated electron flux linearly by using pulse widths where $\Delta T_B \leq 1/5$ or we can change the injection level vs. integrated electron flux nonlinearly by using pulse widths where $\Delta T_B > 1/5 \tau$.

Let us suppose that there exists a transient damage process, due to the electron beam, with a lifetime long compared to the longest electron beam pulse duration (4.5 μsec). Then the amount of transient damage generated by the electron pulse will always be directly proportional to the integrated electron beam flux. Thus by using differing beam pulse durations and intensities we can vary the amount of this presumed transient radiation damage while keeping the injection level ($\frac{\Delta n}{n}$) constant. (Or, on the other hand we can keep the damage constant while varying the injection level.)

Figures 10 and 14 are examples of this type of experiment. Since the experimental error in τ is as much as 10% it is uncertain that any difference in τ for differing beam pulse durations exists. The calculated result in Fig. 16 shows us that the single vacancy (a possible lifetime-changing transient-damage) anneals at room temperature within several microseconds. In order to see an effect on τ due to vacancies by this method one would have to perform irradiations at 100° to 150^oK. Our first experiment was done initially at room temperature because this is of largest

interest to device operation.

To get a quantitative idea of the way that damage can vary by this method the following analysis is applicable.

define: g_C = generation rate for carriers by electron beam.

g_D = generation rate for damage by electron beam.

N_C = density of excess carriers

N_D = density of damage (defects/cm^3)

δ_C = fraction decay rate for carriers

δ_D = fraction decayrate for damage

Assume δ_C and δ_D are constant

then we can write

$$\frac{dN_c}{dt} = g_c - \delta_c N_c \qquad \frac{dN_D}{dt} = g_D - \delta_D N_D \tag{9}$$

During beam flux incidence, t = 0 to t = ΔT_B.

$$N_c = \frac{g_c}{\delta_c} - \frac{g_c}{\delta_c} \exp(-\delta_c t) \qquad N_D = \frac{g_D}{\delta_D} - \frac{g_D}{\delta_D} \exp(-\delta_D t) \tag{10}$$

after the beam flux incidence, $g_C = g_D = 0$, and

$$N_c = N_c(\Delta T_B) \exp(\Delta T_B - t)\delta_c \qquad N_D = N_D(\Delta T_B) \exp(\Delta T_B - t)\delta_D \tag{11}$$

where $N(\Delta T_B)$ is obtained from Eq. 10. We can define: $\tau_c \equiv \delta_c^{-1}, \tau_D \equiv \delta_D^{-1}$ and which makes τ_C the lifetime of excess carriers and τ_D the lifetime for damage. We then have

$$N_c = g_c\tau_c - g_c\tau_c \exp\left(-\frac{t}{\tau_c}\right) \qquad N_D = g_D\tau_D - g_D\tau_D \exp\left(-\frac{t}{\tau_D}\right) \tag{12}$$

Using Eq.12 to calculate N_C and N_D immediately after the end of flux incidence (at t = ΔT_B) we get:

(Assume $0.5\ \mu sec \leq \tau_C \leq 3\ \mu sec \qquad \tau_D \geq 50\ \mu sec$)

$$N_{C\,0.1}(\Delta T_B = 0.1) \simeq 0.1\, g_{C(0.1)} \qquad N_D = 0.1\, g_{D(0.1)} \tag{13}$$

$$N_{C\,4.5}\,(\Delta T_B = 4.5) \simeq g_{C(4.5)}\tau_C \qquad N_D = 4.5\, g_{D(4.5)} \tag{14}$$

We adjust $g_{C\ 0.1}$ and $g_{C\ 4.5}$ so that

$N_{C\ 0.1} = N_{C\ 4.5}$ (i.e., equal excess carrier injection levels)

This is done by changing the beam current of the 4.5 μsec pulse relative to the 0.1 μsec pulse. We know that $g_C \propto$ flux rate $\propto g_D$ thus implying $g_{C\ 0.1} = K\, g_{D\ 0.1}$ (K is a constant)

and $g_{C\ 4.5} = K\, g_{D\ 4.5}$.

At $t = \Delta T_B$ we get

$$\frac{N_{D\,0.1}}{N_{D\,4.5}} = \frac{(g_{D\,0.1})(0.1)}{(g_{D\,4.5})(4.5)} = \frac{g_{C\,0.1}\,(0.1)}{g_{C\,4.5}\,(4.5)} \tag{15}$$

but from $g_{C\ 4.5}\,\tau_C = 0.1\, g_{C\ 0.1}$

Therefore

$$\frac{N_{D\,0.1}}{N_{D\,4.5}} = \frac{\tau_C}{4.5} \tag{16}$$

for $.5 \leq \tau_C \leq 3$

Thus we have shown that by changing electron beam pulse widths and keeping the injection level constant we can vary the transient damage density. Therefore on a plot of τ vs Δn (or equivalently τ vs. $\Delta\sigma/\sigma$) one can look for a change in τ due to transient damage independent of the injection level dependence.

VI. Conclusions

1. The increase of lifetime on injection level has been observed in all silicon samples studied, and the observed linear dependence of lifetime on injection level indicates a single

recombination level predominates.

2. No long decay times indicative of trapping were observed in the samples studied.

3. Using the equation for the Hall field set up when one has mixed conduction by electrons and holes it is possible to calculate the approximate shape of the Hall voltage response in 100 ohm-cm p-type silicon which shows a transient conversion to n-type conduction immediately after a pulse of electrons strikes the sample and finally reverts to p-type.

4. A simple calculation which accounts for the ionization energy loss in silicon by ion-pair formation yields within a factor of 2 the dependence of induced excess carriers on electron beam intensity; and the temperature dependence is as predicted by the theory of Appel,[5] additional comparison of more accurate experimental data with theory is necessary before a precise conclusion can be made.

5. A simple model for the fast annealing of 45-50 MeV electron-induced displacement type defects in silicon indicates that, at temperatures of 300°K and above, less than 2% of the damage remains 1 microsecond after the beam pulse strikes the sample. The results of this model together with the experimental findings lead to the conclusion that the significant transient radiation damage process in 45-50 MeV pulsed electron-irradiated silicon is a transient ionization effect.

6. The damage induced by a single pulse of electrons is too low to be detected by conductivity and Hall voltage measurement,

but may possibly be observed in lifetime decay constant changes by irradiating at $\approx 150^{o}K$ (n-type) and $\approx 190^{o}K$ (p-type) as predicted by the annealing model results.

VII. Recommendations and Suggestions for Future Experiments

VII.a.

Our experiments have shown that there is a dependence of lifetime on injection level. We have also seen that the Hall voltage does not decay exactly as expected under assumptions of a single recombination lifetime. In fact, it appears that holes and electrons exhibit differing lifetimes. Our theoretical Hall voltage curve in p-type silicon is based on a constant lifetime τ. If we could get a measure of τ at the beginning of excess carrier decay, a more accurate picture of the decay scheme would emerge. We would also be able to measure τ immediately following the electron irradiation instead of waiting until voltage "saturation" had decayed; this would give a more accurate picture of τ vs. Δn effects. So it is suggested for future experiments that a pulsed exponentially decaying current be supplied to the sample at the end of a beam pulse. The results would be analyzed for n type as follows (p type is very similar),

$$V_\rho = \frac{KI}{\sigma}$$

Where K is a constant depending on sample geometry and I is current through sample.

$$\sigma \equiv e(n_o \mu_n + \Delta n \mu_n + \Delta p \mu_p)$$

But, for large injection we have,

$$\Delta n \gg n_o \qquad \Delta p \gg n_o \qquad \mu_p \simeq 1/3\, \mu_n$$

And we shall assume,

$$\Delta n = (\Delta n)_o \exp(-t/\tau_n) \qquad \Delta p = (\Delta p)_o \exp(-t/\tau_p)$$

Which gives us

$$\sigma \simeq e\left[\mu_n(\Delta n)_o \exp(-t/\tau_n) + \mu_p(\Delta p)_o \exp(-t/\tau_p)\right]$$

Let us define

$$\tau_n \equiv \tau_p + \delta\tau$$

And we shall make an assumption which appears reasonable according to our past experiments.

Assume $\dfrac{\delta\tau}{\tau_p} \leq 0.1$

Therefore we can write for V_ρ ,

$$V_\rho \simeq \frac{KI}{e}\left[\mu_n(\Delta n)_o \exp\left\{-t\left(\frac{1}{\tau_p} - \frac{\delta\tau}{\tau_p^2}\right)\right\} + \mu_p(\Delta p)_o \exp(-t/\tau_p)\right]$$

If we write, $I = I_o \exp(-t/\tau_I)$

Where τ_I is the decay constant for the sample current and is controlled by the experimenter.

Then, $$V_\rho = \frac{KI_o}{e} \exp\left(\frac{t}{\tau_p} - \frac{t}{\tau_I}\right)\left((\Delta p)_o \mu_p + \mu_n(\Delta n)_o \exp t\frac{\delta\tau}{\tau_p^2}\right)^{-1}$$

And for the special case where $\tau_I = \tau_p$ and $\delta\tau = 0$

$$V_\rho = \frac{KI_o}{e}\left(\mu_n(\Delta n)_o + \mu_p(\Delta p)_o\right) = \text{constant.}$$

By varying τ_I so that V_ρ = constant we can get a very good measure of $\tau = \tau_p = \tau_n$.

There is another very important question which this pulsed sample current method will help to answer as the next paragraph will show.

Shockley-Read theory predicts a linear relation between τ and Δn. Our data shows roughly this trend but it does not show it in a way which is directly applicable to the theory. That is because for all cases where $\frac{\Delta\rho}{\rho} \geq 50\%$ the lifetime was not measured until Δn had decayed to the number $(n = n_o + \Delta n)$ at which $\frac{\Delta\rho}{\rho} = 50\%$. In other words, the lifetime τ was measured in the vicinity of the point on the V_ρ vs. t curve at which $\frac{\Delta V_\rho}{V_\rho} = 50\%$ for all large injection cases $((\Delta n)_o \geq n_o)$. Shockley-Read theory would predict τ = constant for all curves where τ was measured at a constant $\frac{\Delta\rho}{\rho}$ point because when $\frac{\Delta\rho}{\rho}$ = a constant, no matter how large $(\Delta n)_o$ (initial excess carriers), the injection level is constant, assuming no transient damage. Therefore, because of the way we measured τ, S.-R. theory predicts no change in τ for $\frac{\Delta\rho}{\rho} \geq 50\%$. Yet our experiment shows that the lifetime continues to increase as $\frac{\Delta\rho}{\rho}$ increases above 50% and furthermore the slope of the line appears to be roughly unchanged for $\frac{\Delta\rho}{\rho} > 50\%$. This effect should be studied in more detail because of its possible implications to the theory. And it would be helpful, in this vein, to know more exactly the lifetime at the beginning of a high injection decay as well as near the end.

VII.b.

The contribution of the surface effects to lifetime are not very certain. Our samples' dimensions were approximately 0.5 cm x 0.2 cm x 0.06 cm, and this small size is expected to lower τ because of surface recombination. This surface problem would tend

to mask bulk effects thus making it difficult to measure transient damage changes in τ. Larger samples should be used in experiments of this kind.

VII.c.

An experiment which was not tried but which would be helpful is to look for impurity effects in injection level vs. flux. Trapping is observable as a decrease in the conductivity expected from a given integrated flux of electrons. Trapping is also observable as an apparent long lived decay in conductivity but this is not so easy to see if the rate of emission from traps to the conduction band is small. Low lying traps would have this property and also they would tend to fill up quite quickly, so at the beginning of the excess carrier decay these traps would show up as a decrease in the excess conductivity expected from the calculated dependence of excess conductivity on integrated beam flux.

VII.d.

The theory by Appel suggests a temperature dependence of induced conductivity vs. integrated flux. Accurate measurements of this effect could be easily taken and compared with Appel's theory.

References

1. J. C. Corelli, A. R. Frederickson, and J. W. Westhead, IEEE Nuclear and Space Radiation Effects Conf. (1966); IEEE Trans. Nucl. Sci., Vol. NS-13, p. 70, Dec. 1966. (Copy of this paper is attached in this report as an Appendix.)

2. First Quarterly Report - ECOM-01788-1, May 1966; Second Quarterly Report - ECOM-01788-2, June 1966; Third Quarterly Report - ECOM-01788-3, September 1966; for research sponsored under contract DA28-043 AMC-01788(E).

3. M. J. Berger and S. M. Seltzer, "Tables of Energy Losses and Ranges of Electrons and Positrons", NASA SP-3012 (1964). (We assumed the ionization energy loss in silicon to be very nearly equal to the energy loss in aluminum.)

4. J. Appel, Phys. Rev. 122, 1760 (1961).

5. J. Appel, Phys. Rev. 125, 1815 (1962).

6. O. L. Curtis, Jr., R. F. Bass, and C. A. Germano, "Impurity Effects in Neutron-Irradiated Silicon and Germanium", Final Report Northrop Nortronics NARD 65-20R.

7. J. A. Baicker, Phys. Rev. 129, 1174 (1963).

8. J. E. Fischer and J. C. Corelli, J. Appl. Phys. 37, 3287 (1966).

9. R. N. Hall, Phys. Rev. 87, 387 (1952).

10. W. Shockley and W. T. Read, Jr., Phys. Rev. 87, 835 (1952).

11. J. S. Blakemore, Phys. Rev. 110, 1301 (1958).

12. B. L. Gregory, J. Appl. Phys. 36, 3765 (1965).

13. B. H. Sander and B. L. Gregory, IEEE Nuclear and Space Radiation Effects Conf. (1966), Palo Alto, California (to appear in IEEE Trans., Dec. 1966).

14. G. D. Watkins, J. Phys. Soc. Japan 18, Supp. II, 22 (1963).

15. G. D. Watkins, Proc. 7th International Conf. on Phys. of Semiconductors, Paris, 1964 (Dunod Cie, Paris, 1965), p. 97.

16. A. H. Kalma, J. C. Corelli, and J. W. Cleland, J. Appl. Phys. 37, 3913 (1966).

References (Cont.)

17. G. D. Watkins, private communication; this data to be published (1966).

18. L. J. Cheng, J. C. Corelli, J. W. Corbett, and G. D. Watkins, to appear in Phys. Rev. (1966).

19. L. J. Cheng and J. C. Corelli, Phys. Rev. 140A, 2130 (1965).

20. J. W. Corbett, "Electron Radiation Damage in Semiconductors and Metals", (1966) Academic Press.

BLOCK DIAGRAM

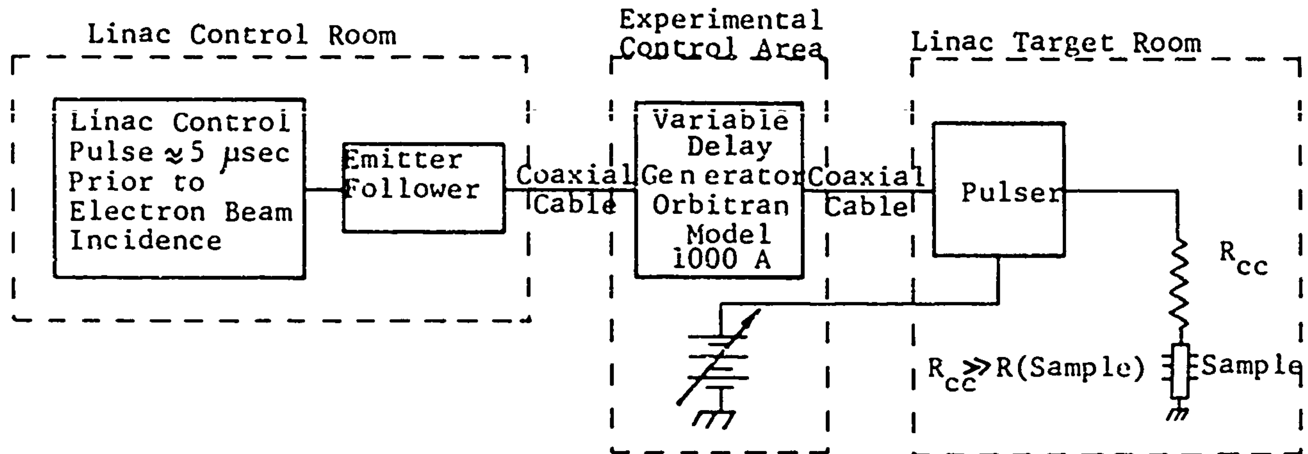

PULSER SCHEMATIC

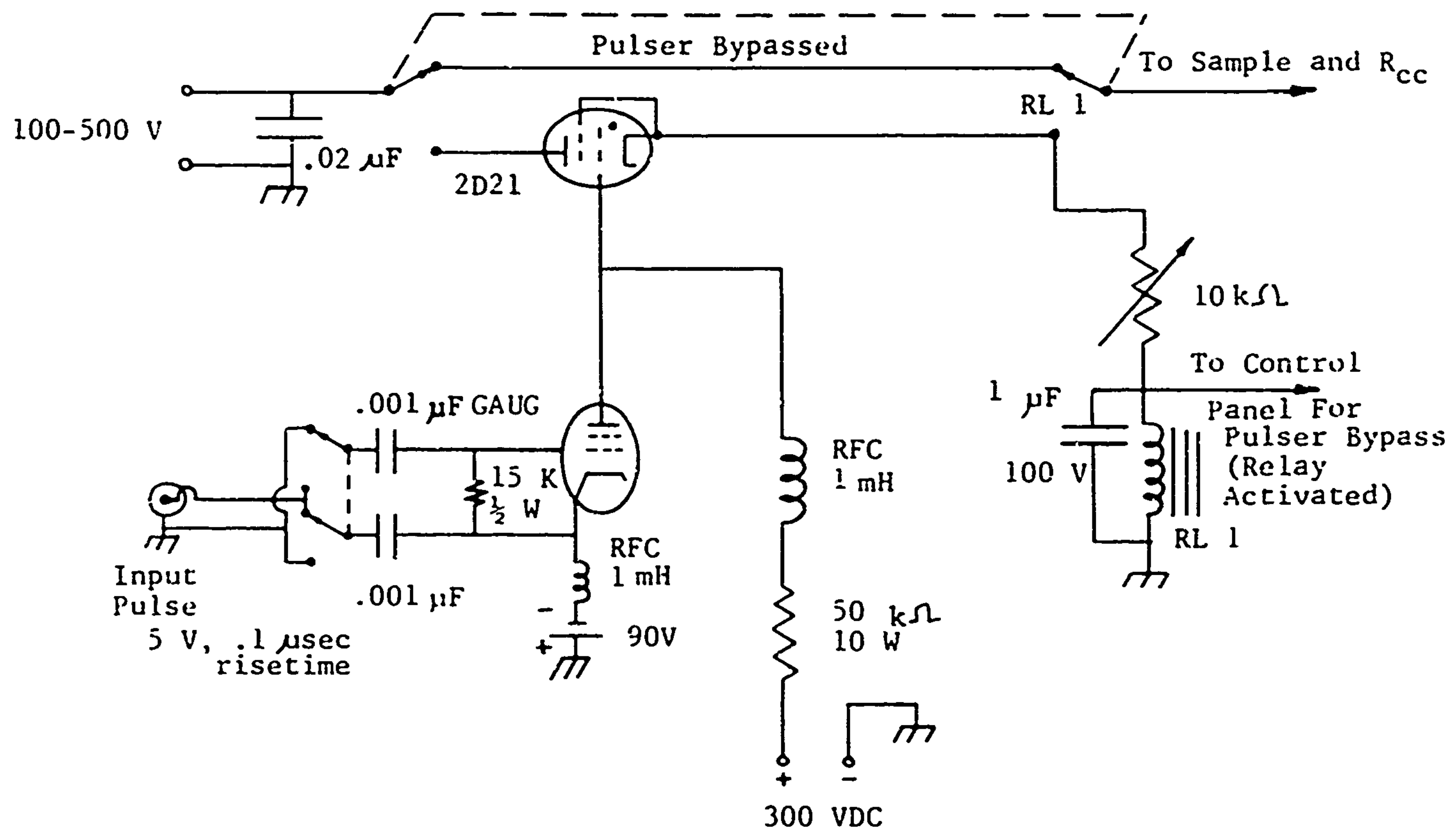

Fig. 1 RL 1 is a 10 kΩ, 100 VDC relay which serves the purpose of turning the pulser off within ½ second after turn on. This prevents excessive IR_S heat build-up in the sample. This delay time is controlled by the 10 kΩ resistor and the 1 μF capacitor. Block diagram of overall electronic system and current pulser schematic circuit diagram showing how pulsed sample current system operates.

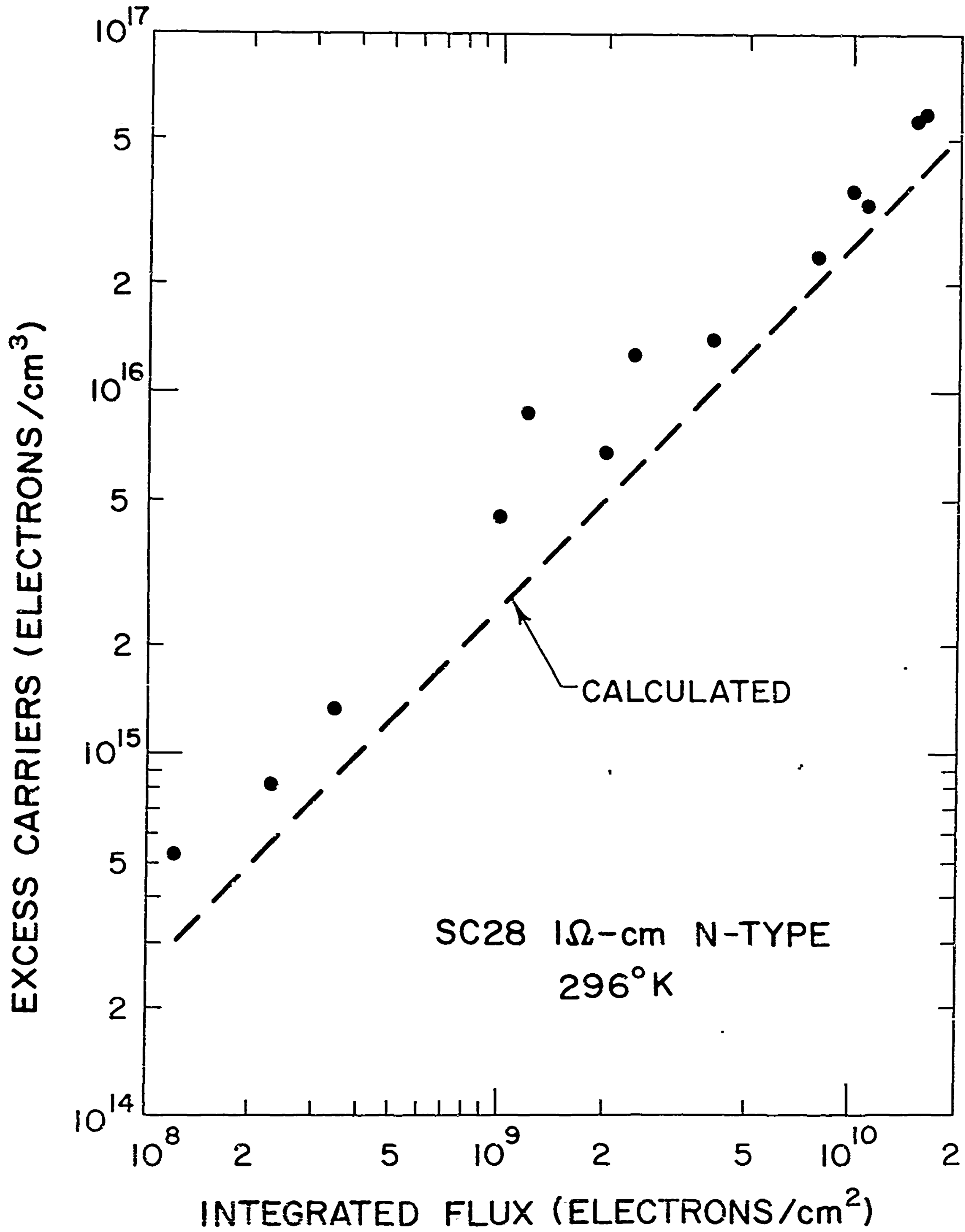

Figure 2

Excess Carrier Generation Vs. Total Integrated Electron Beam Flux

Nominal Error ± 30% Both Scales

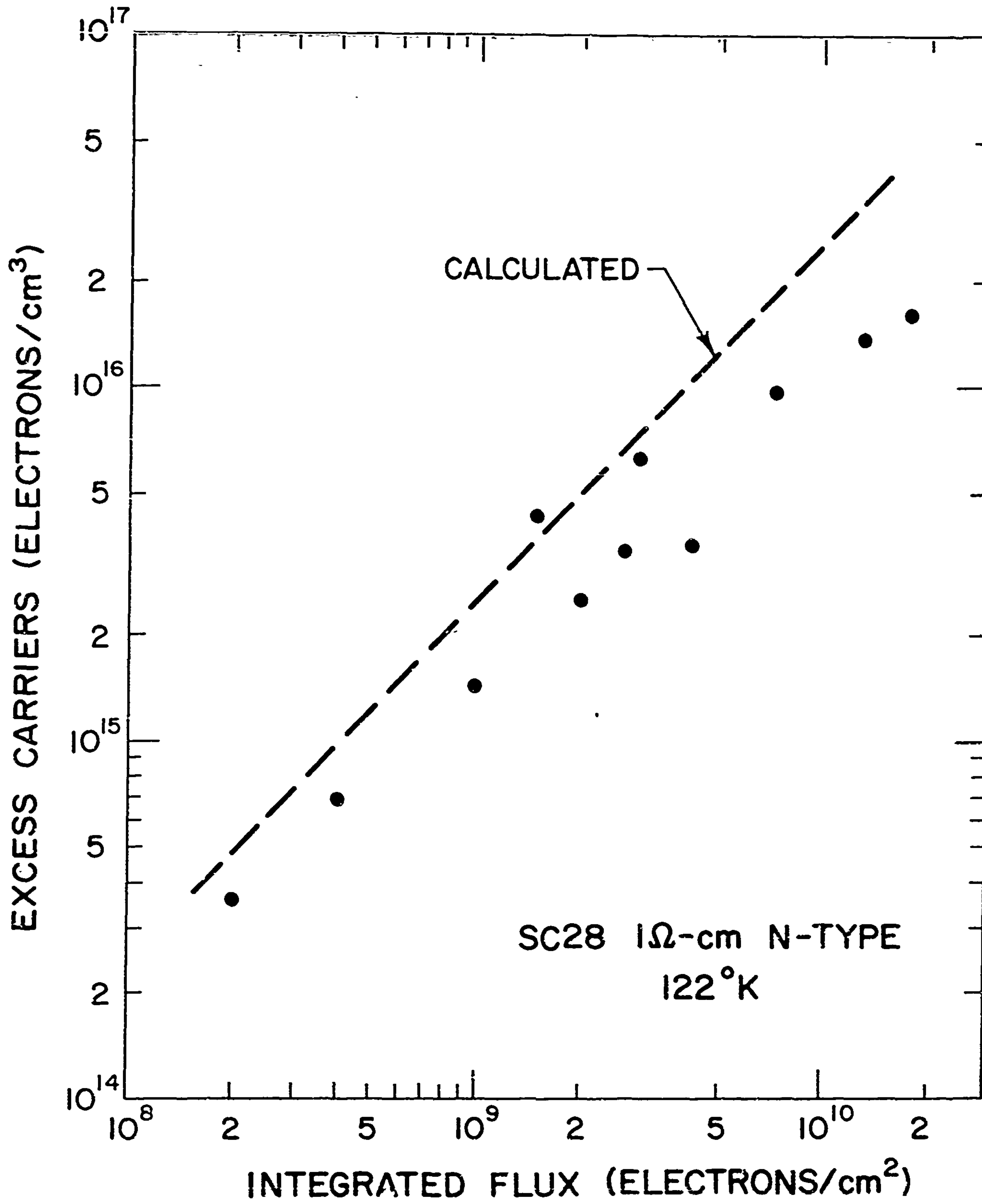

Figure 3

Excess Carrier Generation Vs. Total Integrated Electron Beam Flux

Nominal Error ± 30% Both Scales

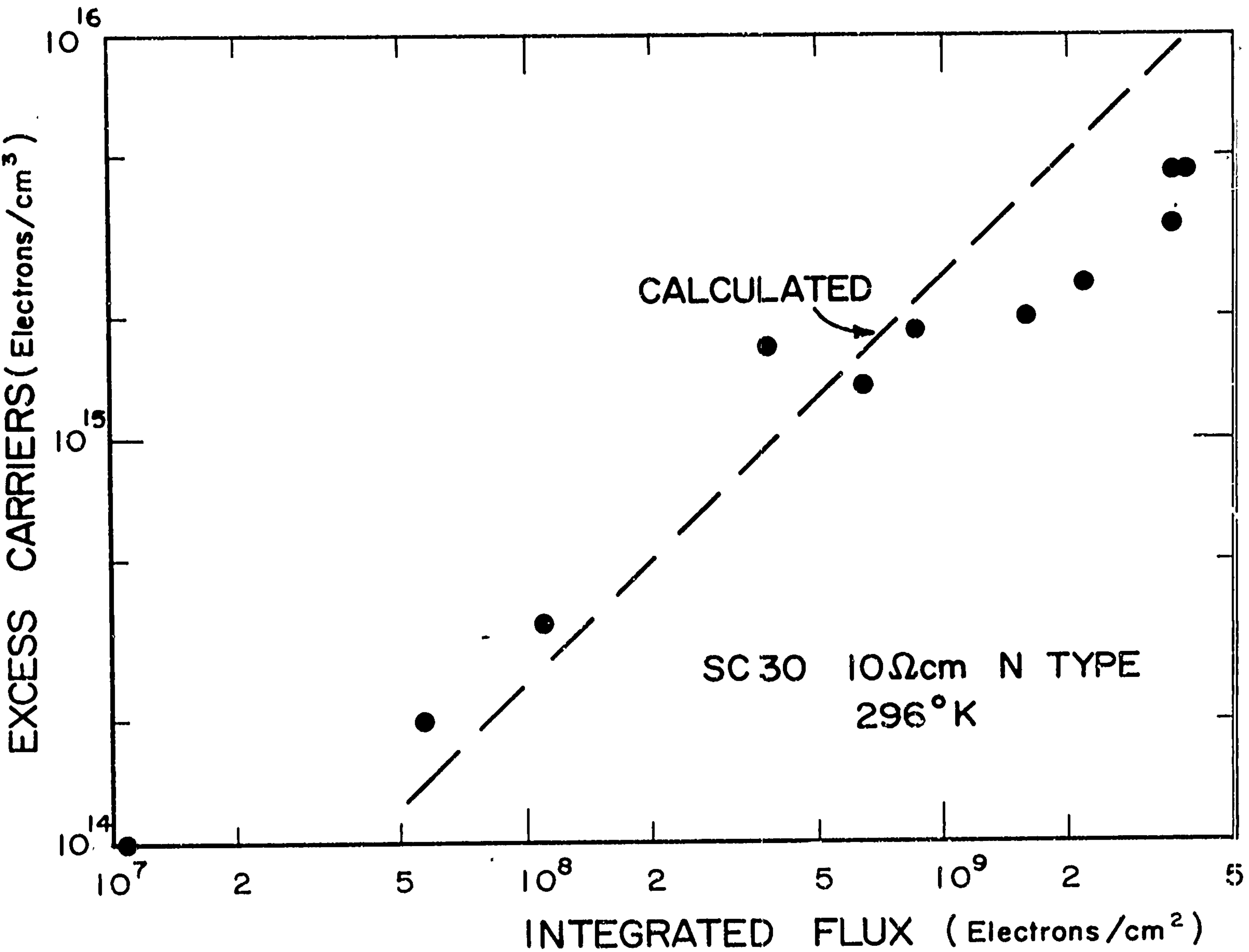

Figure 4

Excess Carrier Generation Vs. Total Integrated Electron Beam Flux
Nominal Error $\pm$ 30% Both Scales

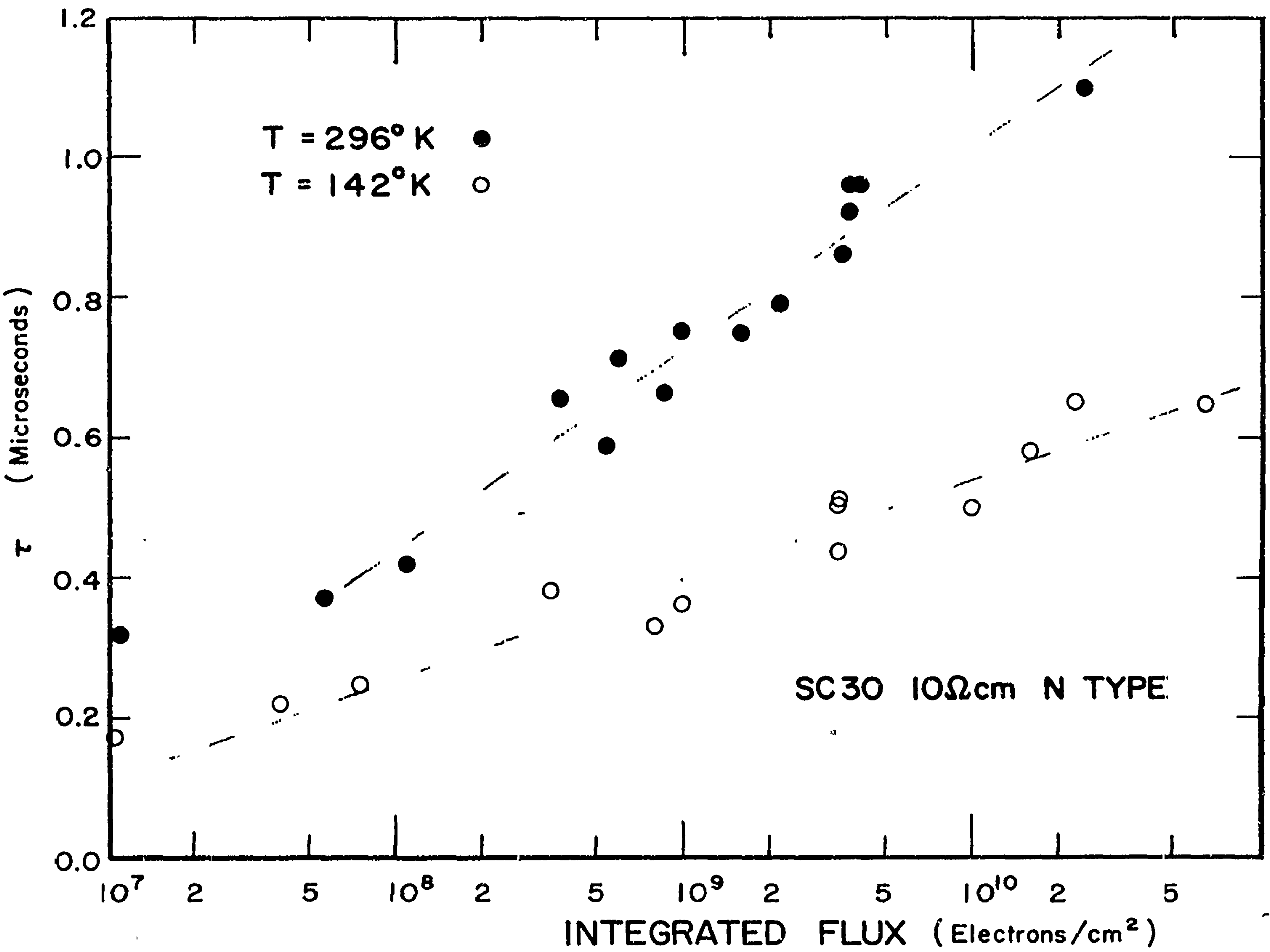

Figure 5 - Excess Carrier Lifetime Vs. Total Flux (Nominal Error ± 30% Flux, ± 10% Lifetime)

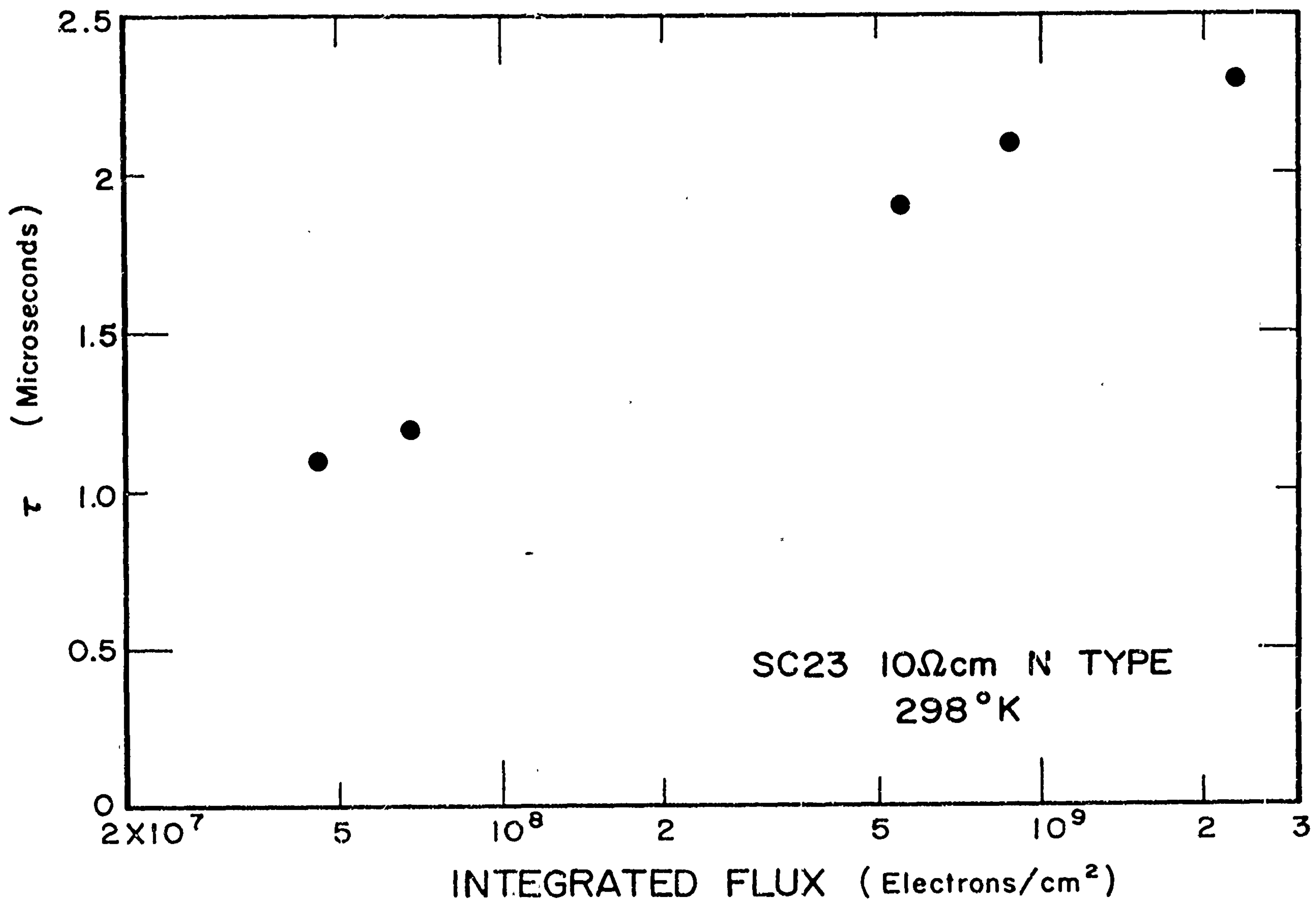

Figure 6

Excess Carrier Lifetime Vs. Total Flux, Nominal Error ± 30% Flux, ± 10% Lifetime

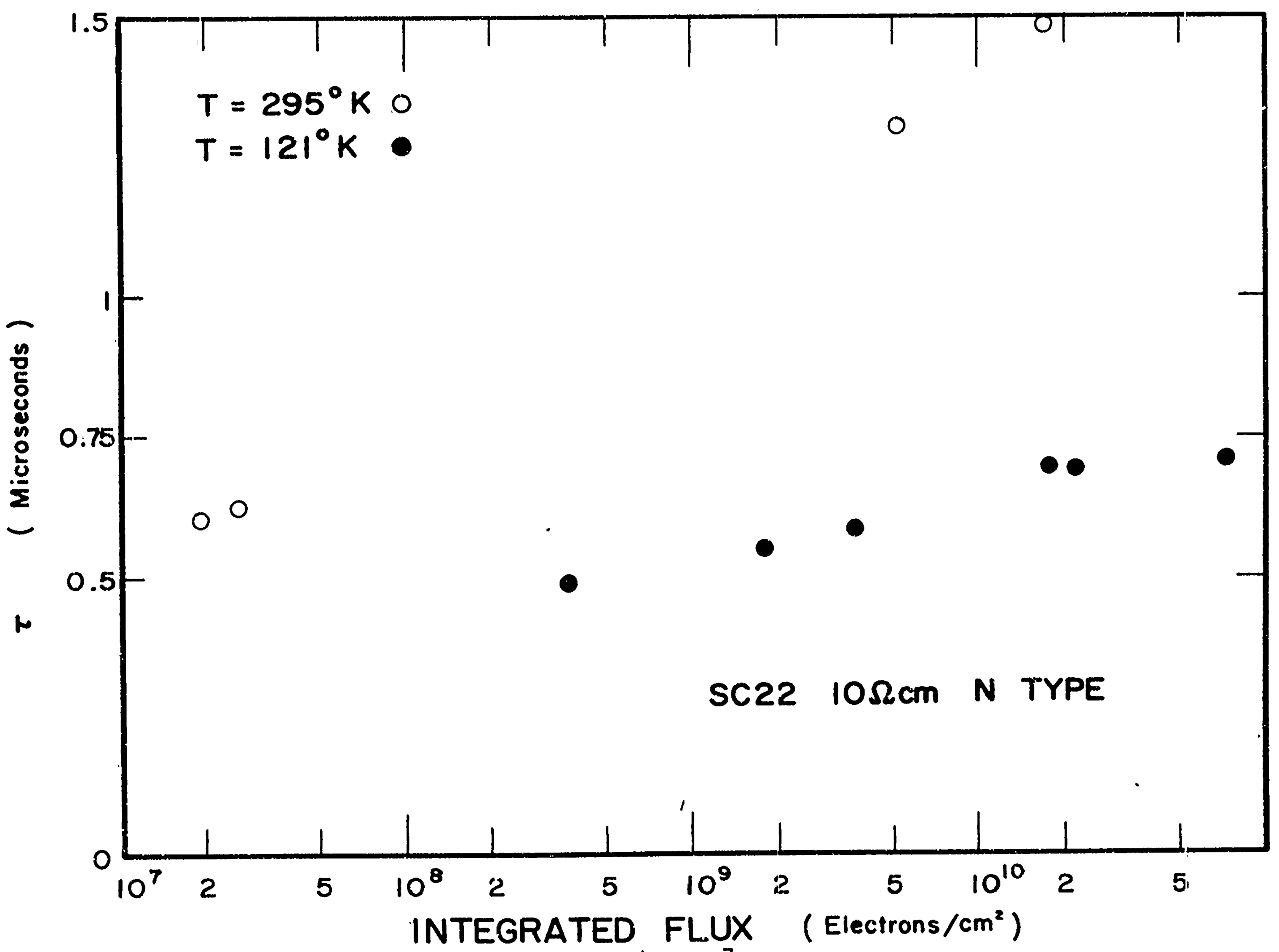

Figure 7

Excess Carrier Lifetime Vs. Total Flux, Nominal Error ± 30% Flux, ± 10% Lifetime

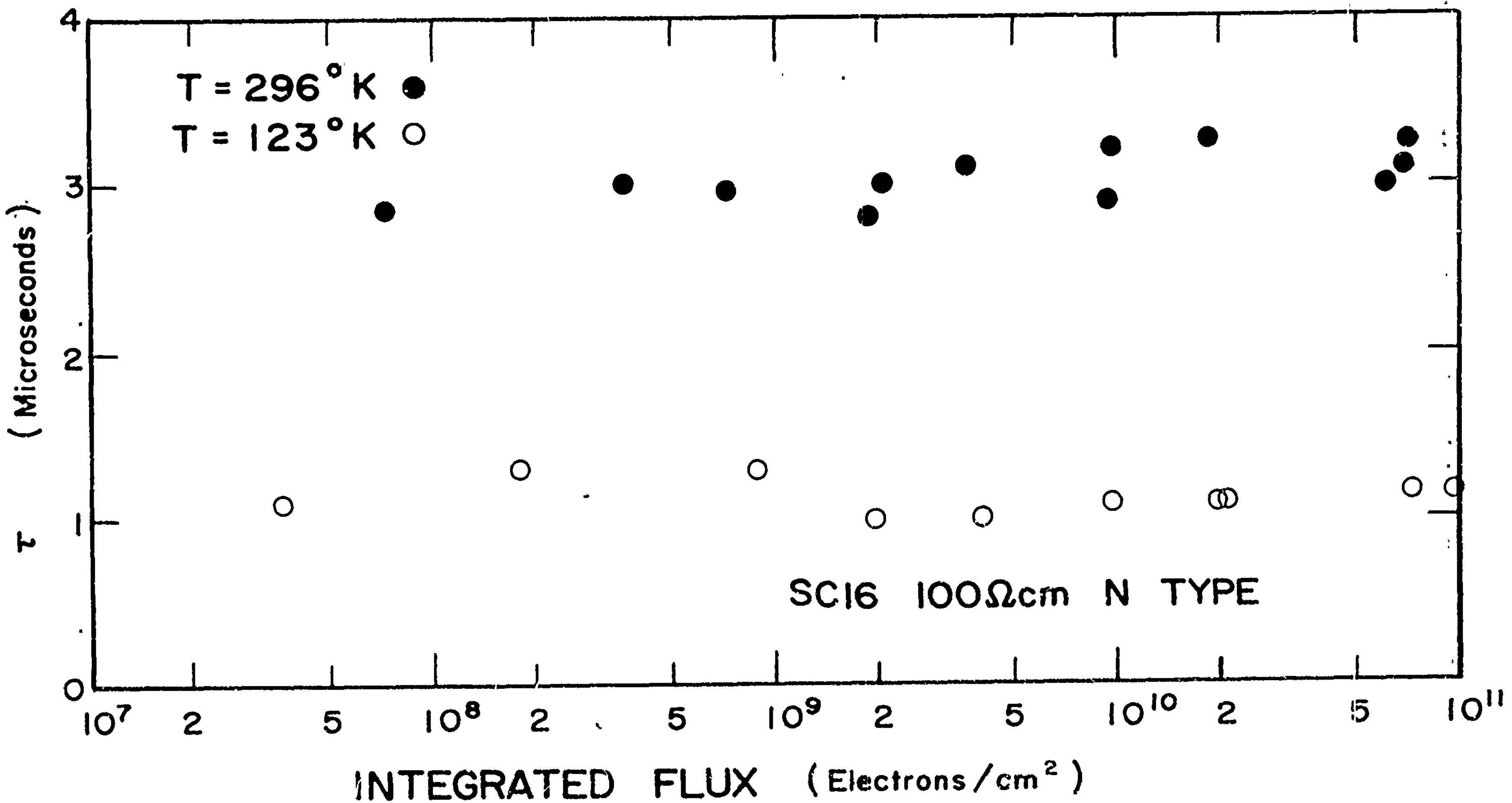

Figure 8

Excess Carrier Lifetime Vs. Total Flux, Nominal Error ± 30% Flux, ± 10% Lifetime

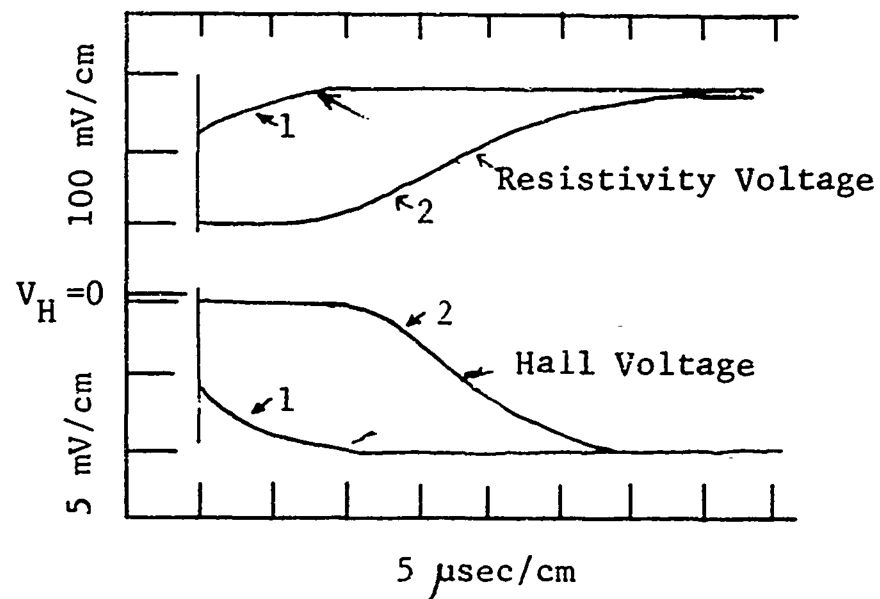

Fig. 9 Transient Hall and resistivity voltage resulting from bombardment of 10 ohm-cm n-type silicon (sample SC-24) by 48 MeV electron pulses of different total dose; for pulses marked 1, dose $\approx 1.9 \times 10^{10}$ e/cm^2; for pulses marked 2, dose $\approx 10^7$ e/cm^2. Sample kept at $\approx 300^oK$ during irradiation.

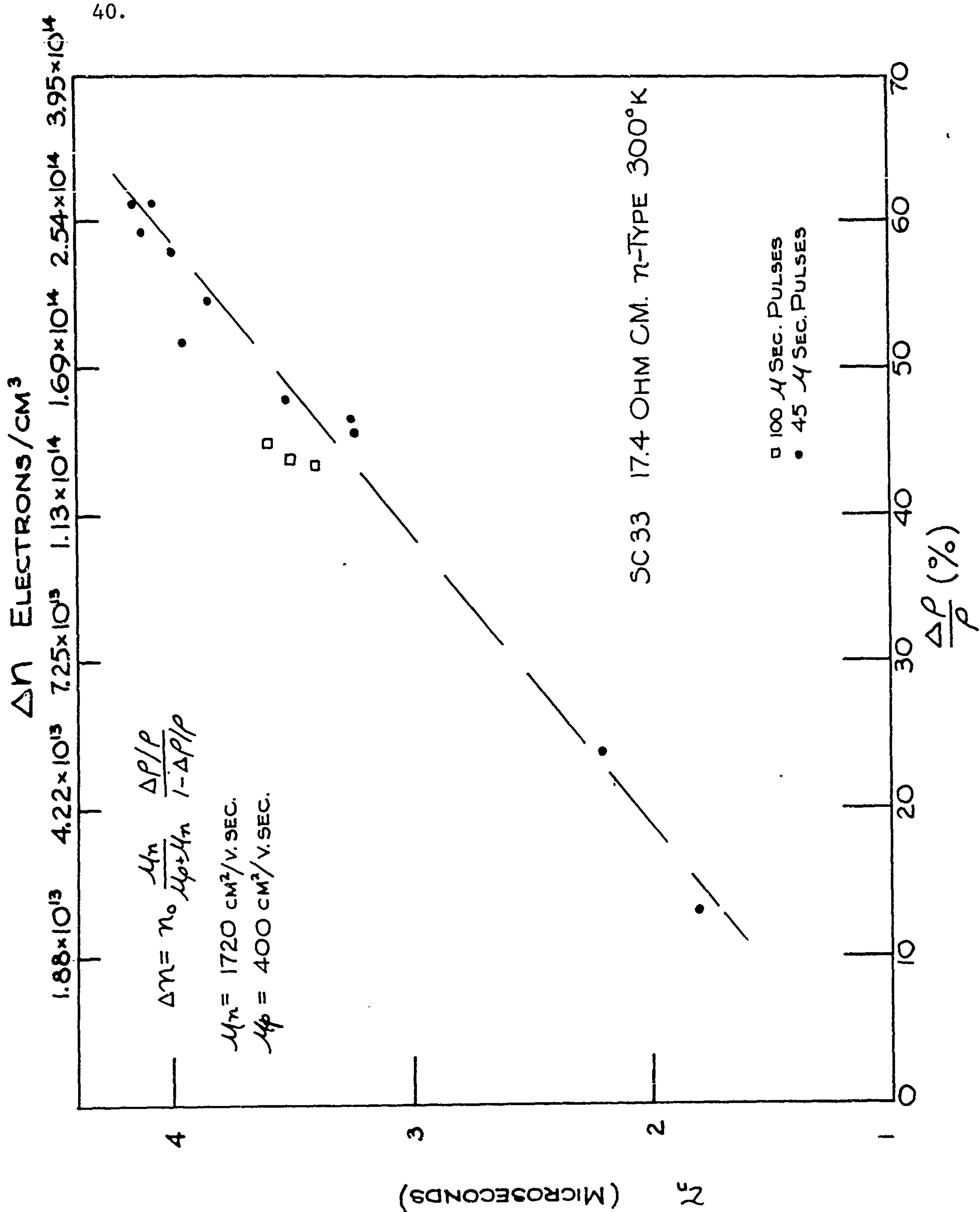

Fig. 10 Dependence of lifetime on injection as measured by injected excess carrier concentration, Δn(electrons/cm^3), or fractional resistivity change $\frac{\Delta\rho}{\rho}$.

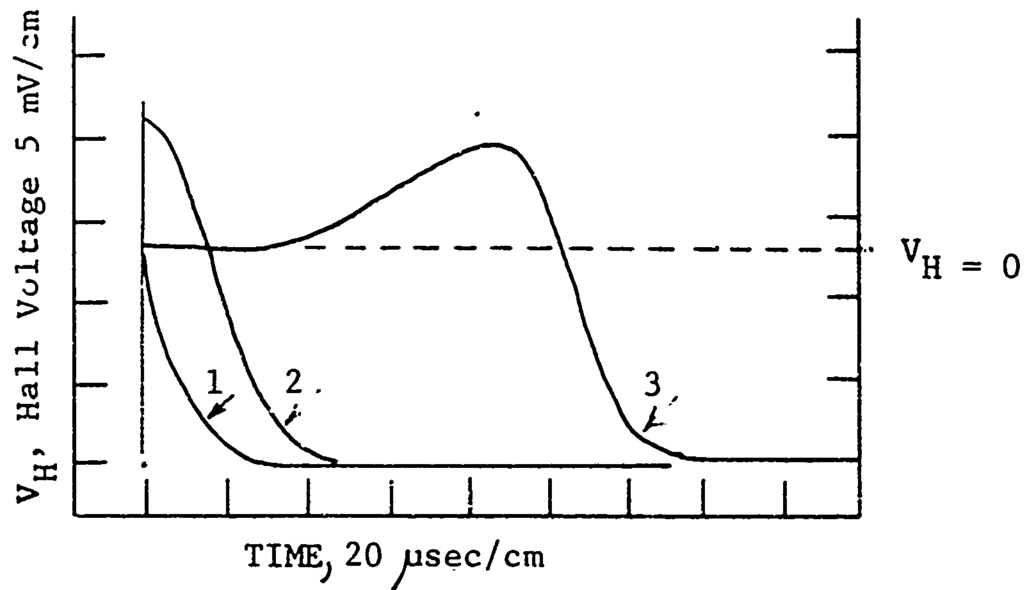

Fig. 11 - Hall voltage response of 100 ohm-cm p-type silicon (sample SC-31) after exposure to 48 MeV electron pulses of three different total integrated fluxes 1 - 4.7×10^6 e/cm^2, 2 - 2.1×10^7 e/cm^2, 3 - 1.3×10^{10} e/cm^2. Sample kept at 300°K during irradiation.

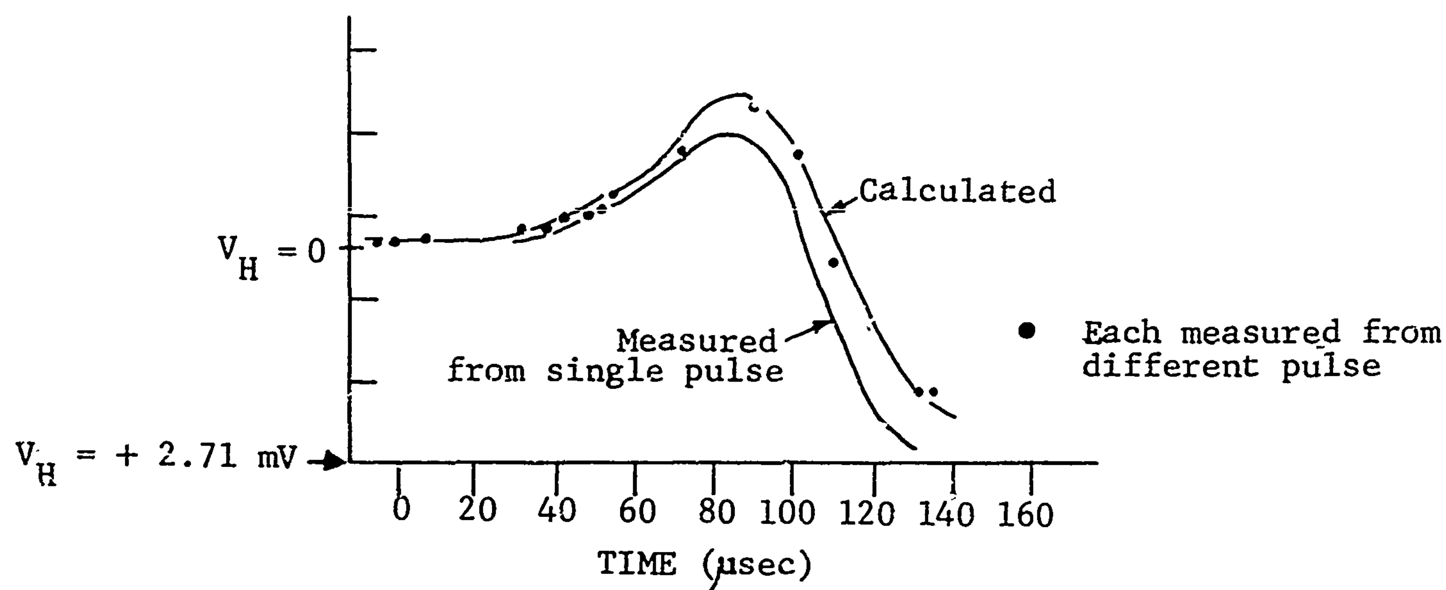

Fig. 12 Comparison of measured and calculated time dependence of Hall voltage for 100 ohm-cm p-type silicon (sample SC-31) irradiated at 300°K by 48 Mev electrons (Dose 1.9 x 10^{10} e/cm^2 for solid line marked measured). For explanation of measured points from different pulses see text.

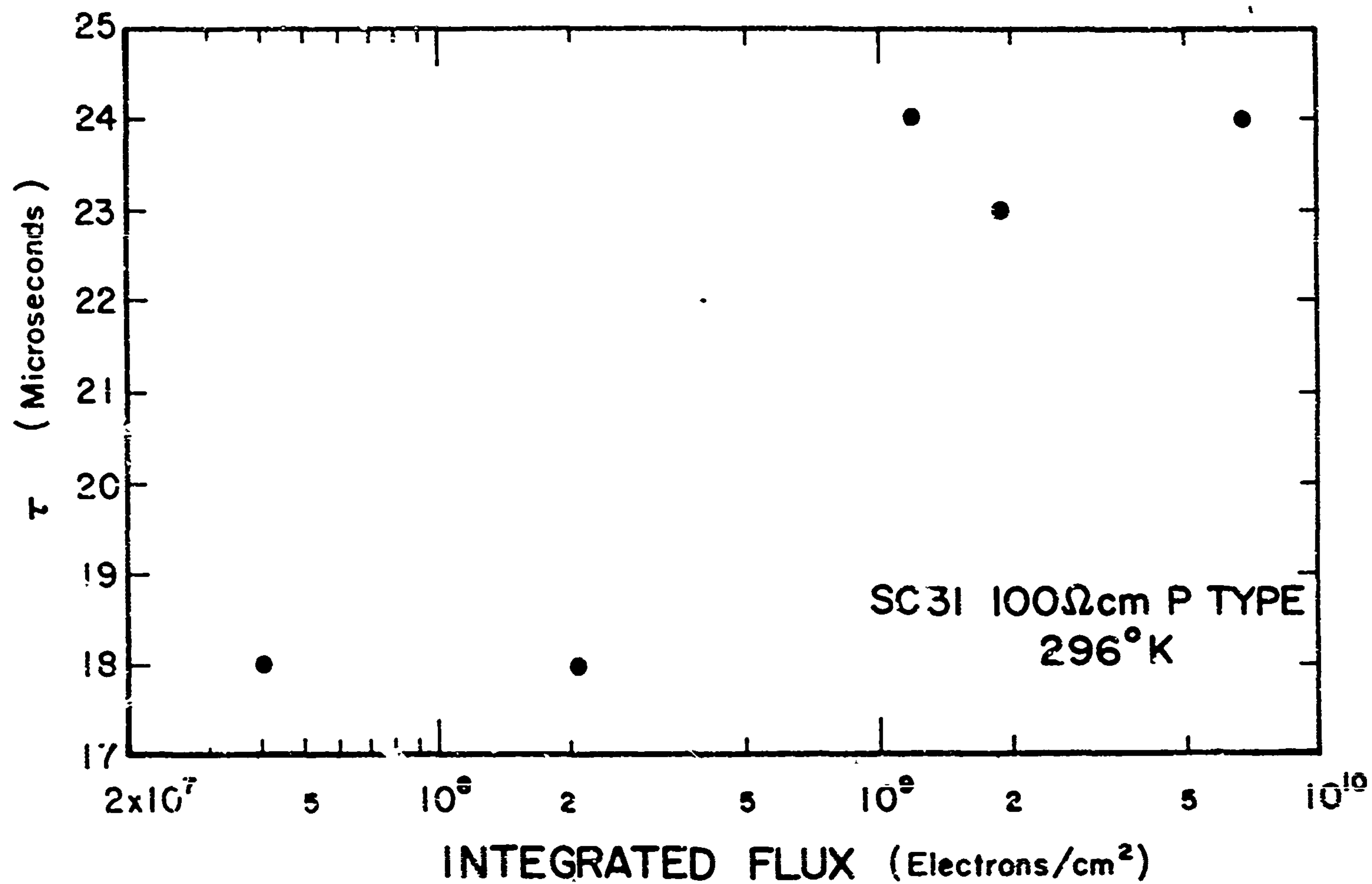

Figure 13

Excess Carrier Lifetime Vs. Total Integrated Flux

Nominal Error: $\pm$ 30% Flux

$\pm$ 10% Lifetime

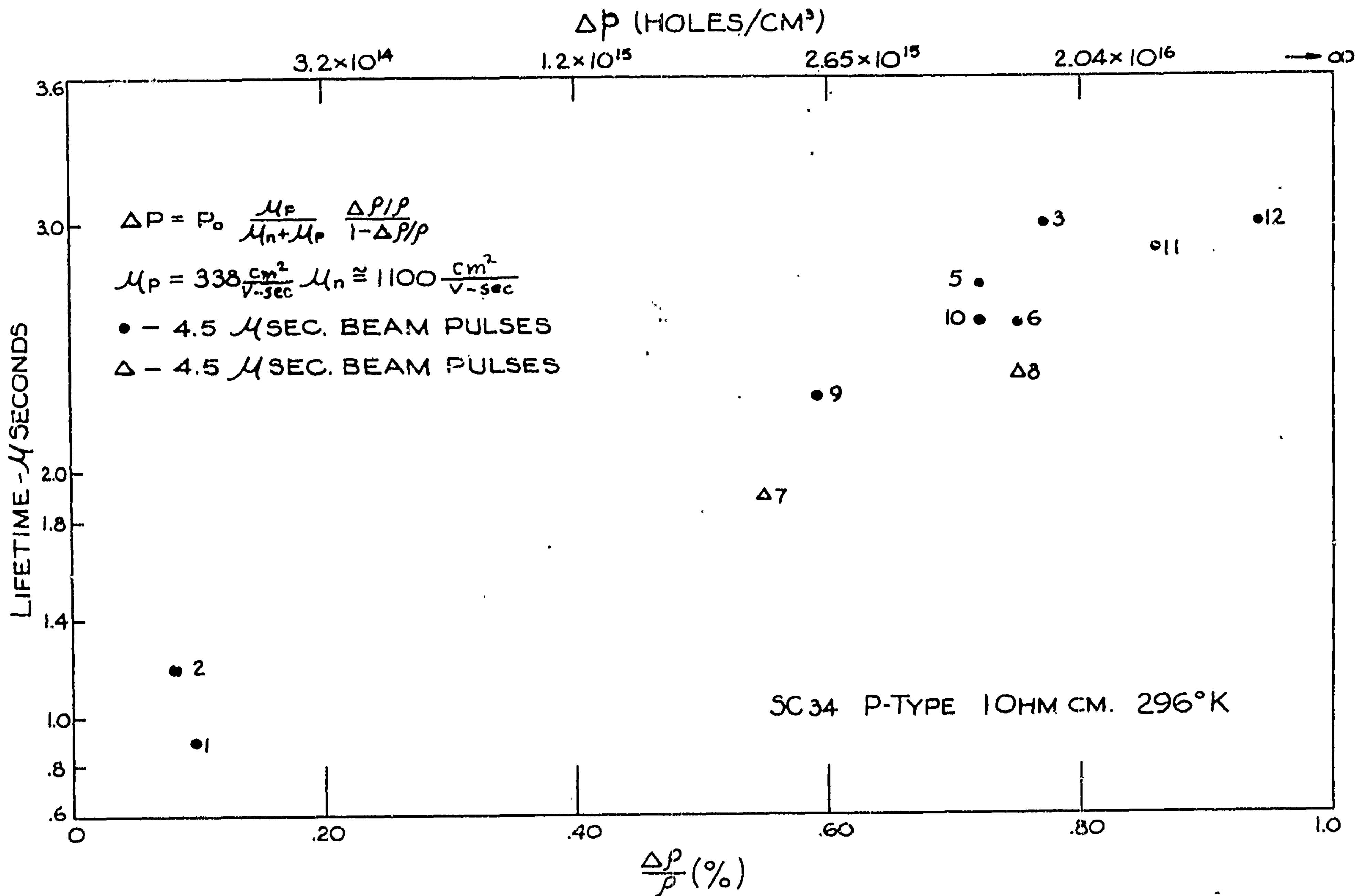

Fig. 14 Dependence of lifetime on injection as measured by excess hole concentration Δp(holes/cm^3) or fractional resistivity change $\Delta\rho/\rho$.

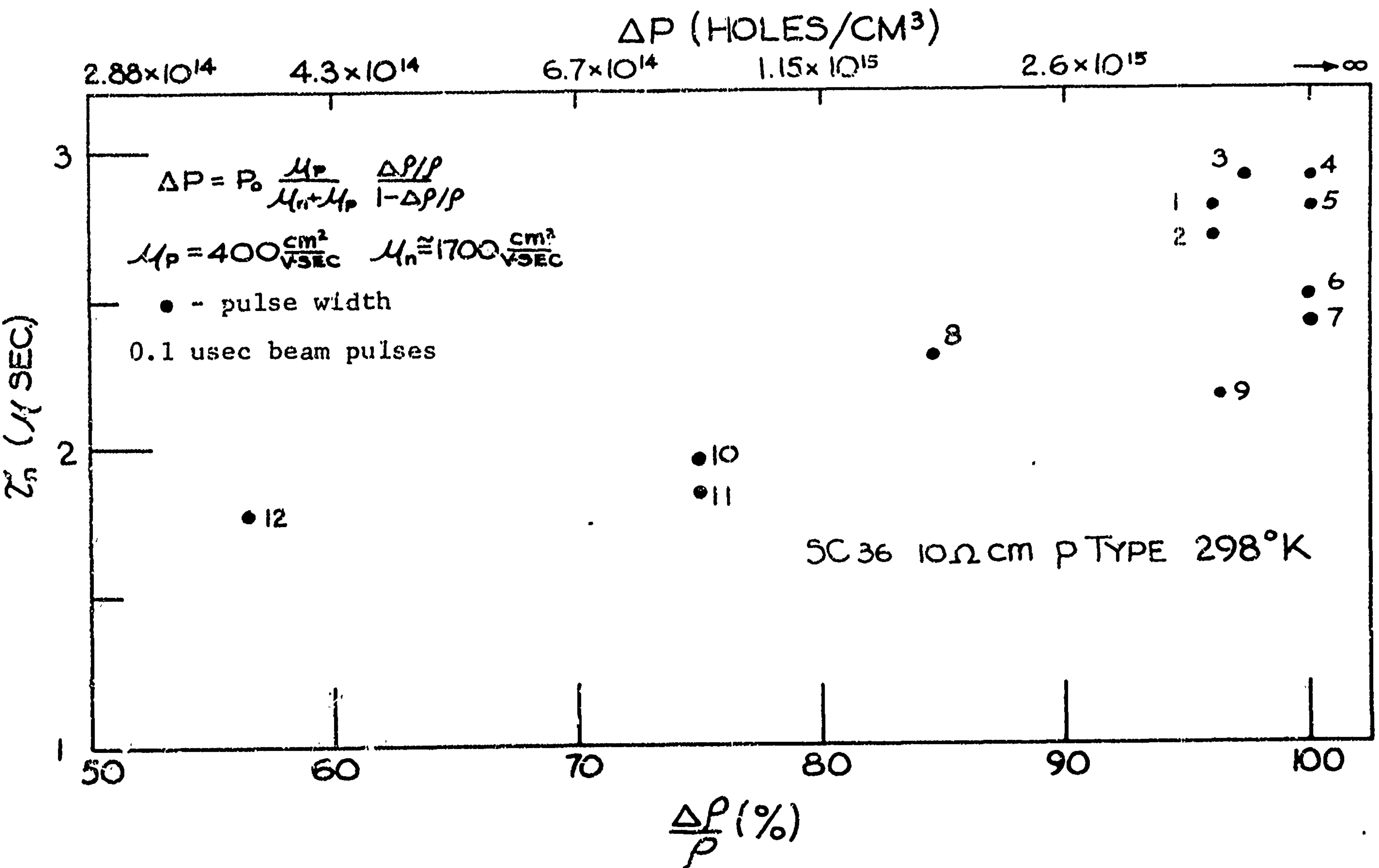

Figure 15

Dependence of lifetime on injection as measured by excess hole concentrations Δp(holes/cm^3) or fractional resistivity change $\Delta\rho/\rho$.

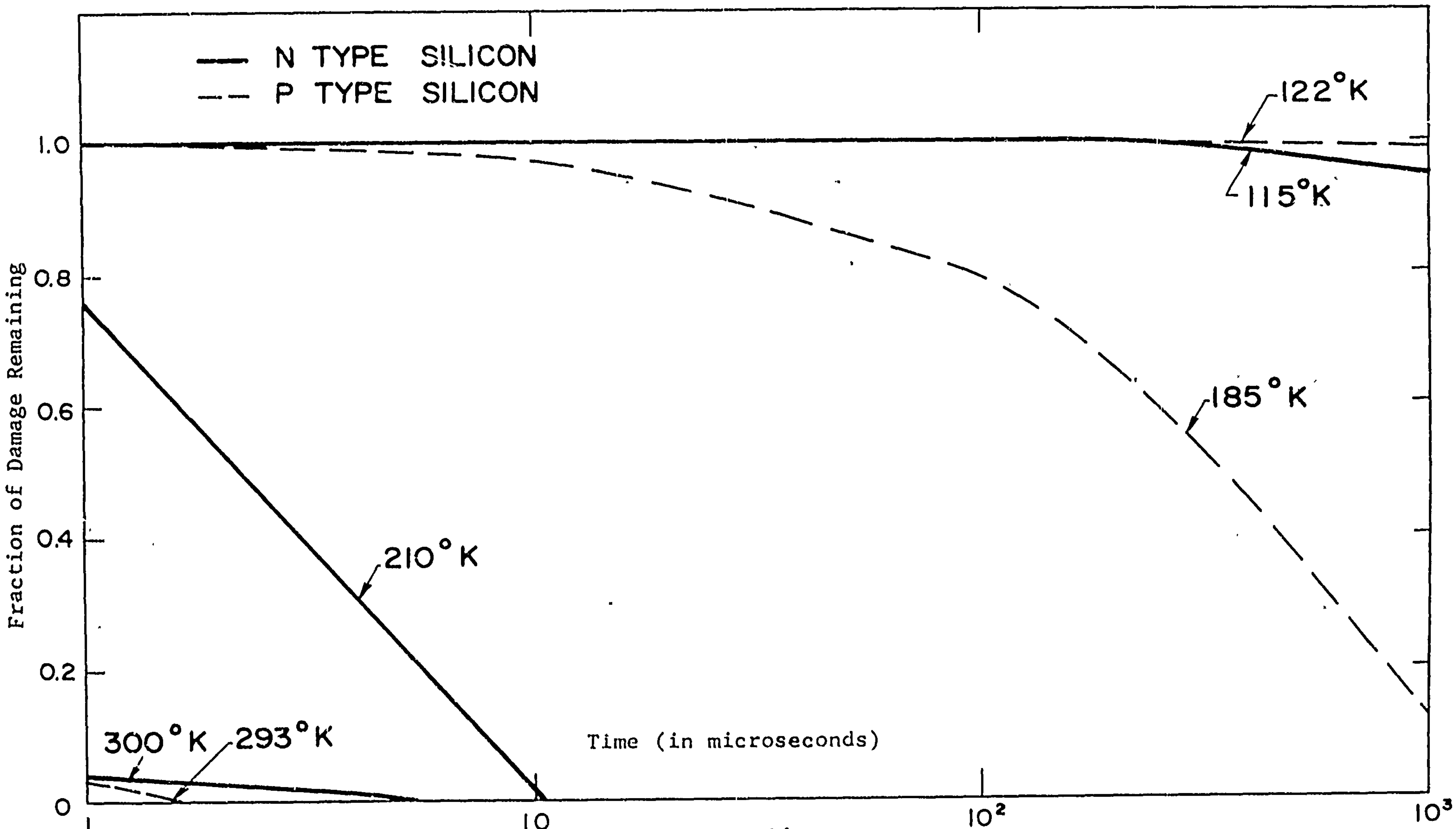

Figure 16

Calculated Fraction of Damage Remaining in n-and p-Type Silicon Vs. Time After Irradiation by 48 MeV Electron Beam Pulses

Appendix

TRANSIENT IONIZATION EFFECTS IN SILICON INDUCED BY 48 MeV ELECTRON PULSES+

J. C. Corelli, A. R. Frederickson and J. W. Westhead
Department of Nuclear Engineering and Science
Rensselaer Polytechnic Institute
Troy, New York

+ Work supported by United States Army Electronics Command, Fort Monmouth, N. J., under Contract No. DA-28-043 AMC-01788(E). Paper to be presented at IEEE Annual Conference on Nuclear and Space Radiation Effects, July 18-22, 1966, Palo Alto, California.

Abstract

Transient radiation effects induced in silicon irradiated in the temperature range 90 to 300°K by 0.007 to 4.5 microsecond pulses of 48 MeV electrons were studied using the transient response of resistivity and Hall effect voltages as the measuring probes. Results are given for one ohm-cm phosphorus-doped n-type silicon and 10 to 100 ohm-cm n-type and p-type samples. In the case of one ohm-cm silicon the results clearly show the actual buildup of excess electrons produced by ionization during the time the electron pulse is irradiating the sample. Moreover, the shape of the pulse during buildup is independent of temperature as long as the electron beam pulse is kept constant. Dependence of the number of injected excess carriers on the ionization intensity (total integrated electron flux in the pulse) was found to be linear up to excess carrier concentrations of $\sim 10^{17}$ cm^{-3}. The lifetime is found to increase linearly with injection implying that the recombination may be dominated by one defect energy level. In p-type silicon the transient Hall and conductivity voltages decay in $\sim$ 20-50 μsec. Relatively long saturation times ($\sim$ 10 to 100 microseconds) are observed in the transient Hall and conductivity voltage following an electron burst. The saturation time decreases with dose accumulation in p-type and also decreases as the irradiation temperature of the sample (both n- and p-type) is decreased. Very similar effects also are observed in n-type silicon samples. In both n- and p-type silicon the Hall and conductivity voltages decay with about the same time constant. Long-

lived resistivity voltage decays were observed in 10 and 100Ω-cm silicon which are due to imperfections (other than radiation-induced) in the crystals. The long lived decay (or the so-called trapping) is observed to last as long as several milliseconds. The significant "damage mechanism" can be understood by considering only the transient ionization effects, since atomic displacements effects are small and insignificant. No fast annealing is observable.

Introduction

The main purpose of this paper is to report on experiments designed to study the effects of a short burst of 48 MeV electrons on the electrical properties of silicon. The changes induced by the radiation pulse in the electrical properties resistivity voltage V_ρ , and Hall effect voltage V_H, are used as the probes for observing the radiation effects. In the experiments conducted thus far one is interested in learning what is occurring in the radiation damage process both during and after the pulse of radiation has struck the sample. In most instances the radiation pulse width ranges from 0.007 to 4.5 microseconds. The research content of this paper is of course in marked contrast to the area of radiation damage research which is concerned with the so-called permanent atomic displacement radiation-induced defects where one studies the radiation effects a long time after the defects are introduced. The displacement type defects have been studied in detail for quite some time and the results are well documented(1). However, there is not a large body of literature on the studies relating to transient radiation effects. It has been only recently within the past six or seven years that the importance to nuclear weapons of the effects of radiation bursts on electronics became an area in which much effort has been concentrated in an attempt to understand the basic mechanisms which obtain in semiconductor devices expected to operate in a pulsed radiation environment.

In this paper we report on experiments in which silicon samples were exposed to 50 MeV electron pulses. The experiments

were designed with the intention of observing fast annealing of atom displacement damage in silicon, and as anticipated the overwhelming dominance of ionization effects made it impossible to observe the much lower probability of atomic displacements. However, it was possible to observe permanent radiation damage from one pulse to the next early in the irradiation of ~100 ohm-cm silicon by noting the decrease in carrier recombination time. In order to assess the effects of impurities (concentration and chemical species) in the transient radiation damage process experiments were performed on silicon samples containing boron, indium and phosphorus to impurity levels ranging from $\sim 10^{13}$ to 10^{16} atoms/cm^3 It is important to consider the effect temperature has on the transient radiation effects and a beginning in this direction was made in the experiments reported on herein by irradiating with the sample temperature maintained at 90°K up to 300°K

Experimental Methods

The samples studied in the irradiation experiments were prepared from silicon wafers 0.030" thick sliced from ingots purchased commercially.* An ultrasonic cutter was then used to cut eight-arm bridge-type samples suitable for conductivity and Hall effect measurements. The bridge samples were etched (3 HNO_3, HF mixture) and then polished to ≈0.025" thickness. The samples were instrumented with electrical contact leads which were stable and ohmic over the temperature range of interest 80-300°K. The sample was irradiated in a liquid nitrogen cryostat capable of

* Pulled silicon purchased from Mallinckrodt Chemical Works, St. Louis, Missouri. Floating zone silicon purchased from Semi-Elements, Inc., Saxonburg, Pa.

maintaining sample temperatures from 80°K up to 350°K. A heater was wound on the copper block to which the sample was attached. Thermometry was accomplished using two copper-constantan thermocouples mounted at the top and bottom of the sample. The sample was in a light-tight and vacuum environment during irradiation. The cryostat was placed in an electromagnet (6500 gauss) which had 1" diameter holes in the pole pieces to allow the electron beam to pass through the sample while Hall effect measurements were being made.

In order to minimize electrical noise pickup it was necessary to conduct voltage signals out of the target room to the readout area by coaxial cables contained in copper pipes which served as shields. This shielding method eliminated much of the rf electrical noise. pickup. The readout equipment consisted of standard oscilloscopes, cameras, amplifiers etc., which recorded the sample resistivity and Hall effect voltage signals and the electron beam current collected in the faraday cup. The faraday cup consists of a solid lead-lined aluminum cylinder which stops and collects the electrons after they pass through the sample. This cylinder is in turn surrounded by and insulated from a hollow metal cylinder. The oscilloscope then measures the current from the beam stop to the outer cylinder which is grounded. The R.P.I. L-band microwave electron linear accelerator operating in the pulsed mode supplied $\approx$48 MeV electron pulses of duration ranging from $\approx$0.007 to 4.5 microseconds. The faraday current collector cup was externally shielded and the signal pickup coaxial cable lead was inserted into a copper pipe in order to allow measurement of low pulse currents ($\sim$5 microamp).

A schematic diagram of the experimental arrangement used in the irradiation experiments is shown in Fig. 1. The electron beam exits from the Linac through the beam port window and strikes an aluminum slab at the entrance hole of the beam collimator. The purpose of the aluminum slab is to serve as a beam homogenizer by electron scattering. The beam passes through a hole in the magnet pole piece and then strikes the sample. The beam is stopped and the beam current collected in the faraday cup.

Experimental Results and Discussion

The samples studied were n-type and p-type silicon doped with boron, indium or phosphorus impurities to resistivities in the range $\gtrsim 1$ to ≈ 100 ohm-cm. Both floating zone and pulled silicon have been studied in an attempt to ascertain the effects, if any, of high oxygen concentration $\gtrsim 10^{17}$ cm^{-3} (pulled) and low oxygen concentration $\lesssim 10^{16}$ cm^{-3} (floating zone) on the transient decay process. A description of all samp[illegible] studied is given in Table I. The resistivity, carrier concentration, and Hall mobility values are from the steady state measurements taken before irradiation at the temperatures shown. Also given in Table I is the sample dopant and code designation. In all pulsed irradiation studies the incident electron energy of ≈ 48 MeV passed through the sample in the $\langle 111 \rangle$ direction. The carrier concentrations given in Table I were calculated from the measured Hall coefficients using $R_H = \frac{r}{ne}$ where R_H is the Hall coefficient, e is the electron charge, n is the number of electrons or holes

per cm^3, and r the ratio of Hall to drift mobility was put equal to unity and its temperature dependence neglected for simplicity.

In order to obtain as much information as possible it is necessary to use a wide range of peak electron beam currents. At the low peak electron beam currents ($<$ 1ma) the linac pulse shape is not "clean" i.e., one having a square top without presence of spikes superimposed on the square top. It is in this electron beam current range that one approaches low injection in the number of excess carriers introduced by ionization and one can measure the low injection recombination rate of electron-hole pairs. Since the electron beam pulse shape for low peak currents contains more noise component than for the high peak currents it is difficult to obtain accurate incident flux measurements, and for this reason the error is larger for our low peak current measurements.

P-type Silicon

In Fig. 2 are shown the transient resistivity voltage pulses for 100 ohm-cm p-type silicon (sample SC-27) which result from irradiating the sample with successively higher peak electron beam currents. The curves shown in Fig. 2 were gotten by tracing the pulse exactly as it was recorded in the polaroid camera film (recall that oscilloscope - camera systems were used to record the pulse data). In all additional results to be presented in this paper the same procedure as outlined above was used to construct curves of the time dependence of resistivity and Hall effect voltage. The voltage measurements shown in Fig. 2 were made with

the sample irradiated at 100°K and 293°K. For each voltage pulse trace shown in Fig. 2 we have given the corresponding total electron dose in the pulse and the quantities $\frac{\Delta\rho}{\rho}$ (note $\frac{\Delta\rho}{\rho} = \frac{\Delta V_{\rho}}{V_{\rho}}$) where $\Delta\rho$ is the incremental change in the electrical resistivity, ρ , produced by the radiation-induced carriers which give rise to a voltage change ΔV_{ρ} . The voltage V_{ρ} is the quiescent dc voltage value across the resistivity leads of the sample before the electron beam pulse is incident on the sample. The pulse shape shown in Fig. 2 for low electron beam peak currents appears to be characteristic of any typical low injection photo-induced excess electron-hole recombination process. The pulse shape exhibits a voltage saturation* as the sample is exposed to the higher doses. More will be said of the saturation effects later. In the p-type silicon results shown in Fig. 2 there is no observed long-lived voltage decay which would be characteristic of trapping processes. From the results given in Fig. 2 one observes that the carrier lifetime (decay) shows a marked increase with increase of injection. The shorter carrier recombination times observed in the 100°K irradiations when compared to the 293°K irradiations represent the normal well known[2,3] temperature dependence of carrier lifetimes in silicon. The carrier lifetimes obtained from the data of Fig. 2 are lower than typically measured values. This is due in most part to the surface recombination which results in a decrease in lifetime because our samples are thin and have a large surface to volume ratio.

---

*This effect arises since a time equal to several lifetimes must elapse after the electron beam pulse in order that the large concentration of excess carriers decrease by recombination thereby yielding an easily measurable voltage change with time.

We can characterize the electron dose[4] which has been delivered to the sample in terms of roentgens as follows: one roentgen (1R) deposits 83 erg in one gram of air at $0^{o}C$ and 760 mm of mercury pressure. Using the tables of Bergen and Seltzer,[5] which give the energy loss by electrons in various media, we compute that (relative to air) 1R is equivalent to $\approx 1.5 \times 10^{7} \frac{e}{cm^{2}}$ for 50 MeV electrons. In Fig. 3 are given the response of the resistivity voltage for 100 ohm-cm p-type silicon (sample SC-18) irradiated at 29[illegible]^{o}K by 48 MeV electron beam pulses of varying pulse widths ranging from 0.01 to 4.5 μsec. Also given in Fig. 3 are the total electron dose in electrons/cm^{2} in the pulse, the corresponding exposure in R, and the exposure rate in R/sec where we have used the method above to transform electron flux to roentgens. In Fig. 3 we observe that for 100 ohm-cm p-type silicon saturation times are long compared to electron beam pulse width. Also shown in Fig. 3 is the dependence of the transient ionization effects on dose rate. The results given in Fig. 3 for electron doses of 10^{10} to 10^{11} electrons/cm^{2} are typical of p-type silicon in the 10 to 100 ohm-cm resistivity range.

In order to check the temperature dependence of the saturation in resistivity voltage, and also to check whether or not long-lived traps ($>$ 50 μsec) are induced at lower temperatures sample SC-18 was irradiated at low temperatures (95 and $185^{o}K$). The results are shown in Fig. 4 where one can observe easily measurable differences in the saturation time in that there exists a

striking decrease in the saturation time (note the different scales) as the sample is irradiated at lower temperature. For example the saturation time in the 95°K irradiation is ≈ 4 μsec while in the 295°K irradiation the saturation time is ≈ 30 μsec. It appears that the decrease in carrier recombination lifetime, well known from other studies in silicon[2] and germanium,[6,7] is important to understand the results given in Fig. 4. It is important to point out that the electron beam pulses (these are also shown in Fig. 4) induce roughly 50 times more excess carriers than are present initially in the sample ($\sim 10^{14}$ cm^{-3}, see Table I), which of course causes the saturation in the voltage.

In Fig. 5 are shown the resistivity voltage pulses for ≈ 80 ohm-cm p-type silicon (sample SC-14) irradiated by 48 MeV electron pulses at 288°K under various conditions of pulse width and sample current. The peak electron beam current was kept constant at about 200 ma for all pulses which corresponds to total integrated electron fluxes in the pulse of $\approx 10^{12}$ electrons/cm^2 for 4.5 μsec pulse width, and $\approx 10^{9}$ electrons/cm^2 for the 0.007 μsec pulse width. In none of the results shown in Fig. 5 do we observe long-lived decays (trapping) lasting longer than 100 μsec. In Fig. 5c are shown the voltage pulses of the sample for the same electron beam pulse (0.01 μsec) but for different dc sample currents. If we take into consideration the saturation effects, the electrical noise and the accuracy of the measurement we can conclude that the peak voltage magnitude is proportional to the sample current. An important observation to be made in Figs. 5a and 5b is the

relatively long saturation time which initially is as high as 100 μsec before the sample has been exposed to subsequent beam pulses. Note the marked decrease in saturation time with dose accumulation (Fig. 5a) due to "permanent" radiation damage probably manifesting itself as recombination centers. Additional evidence for the radiation-induced decrease in saturation time with dose accumulation for $\approx$ 80 ohm-cm p-type silicon is shown for sample SC-18 in Fig. 6. The electron beam pulses are also shown in Fig. 6.

Transient Hall effect voltage measurements were made during and following pulsed irradiation (48 MeV electrons) of 80 ohm-cm p-type silicon sample SC-31. The irradiations were performed with the sample kept at 122°K and at 296°K. One would expect to observe a conversion of conduction from p-type to n-type during the time the radiation-induced excess electrons are present in the sample in larger concentration than the initial p-type dopant in the sample having boron concentration $\approx 2 \times 10^{14}$ cm^{-3}. That this is indeed what happens is demonstrated by the results for sample SC-31 given in Fig. 7, where we have shown how the radiation induced excess electron concentration causes the Hall effect voltage to go from p- to n-type in sign. The pulse shapes in Fig. 7 can be approximately reproduced by calculation using the expression for the Hall field, E_H, for mixed electron-hole conduction given by

$$E_H = \frac{JB}{e} \frac{p(t)\mu_h^2 - n(t)\mu_n^2}{[p(t)\mu_h + n(t)\mu_n]^2}$$

where J and B are the current and magnetic flux densities respectively and all other symbols have their usual meaning. In the calculation we assume constant mobility and a single exponential decay of carrier concentration $n(t)$ and $p(t)$ with time.

n-type Silicon

Two samples of n-type silicon 10 ohm-cm (floating zone) were cut from different portions of the same ingot, sample SC-11 and sample SC-21. Some typical transient responses of the resistivity voltages, ΔV_p, following $\approx$48 Mev electron beam pulses are shown in Fig. 8. The temperature of the samples (SC-8 and SC-11) during irradiation and the electron beam pulse characteristics are also given in Fig. 8. A rather striking observation can be made from the results of Fig. 8 in that a relatively long-lived component of voltage persists for times that are very long compared to the electron beam pulse duration. Note that the long-lived component becomes more predominant as the sample temperature during irradiation is lowered. This long-lived decay has been observed in carrier lifetime studies in silicon(2) and germanium(7) and is attributed to defects which act as trapping centers and keep excess electrons immobilized for long times before releasing them to recombine with holes. The long-lived decay is believed to be due to trapping centers which are not induced by radiation, the reason for this being that in transient radiation damage experiments run on samples of similar resistivity (10 and 100 ohm-cm) cut from the same two ingots we did not observe trapping. Further substantiation of this result was deduced by the observations that samples SC-8 and SC-11 exhibited a larger concentration of trapping centers(8) than the other samples cut from the same ingots.

Whenever traps are observed in either n-type silicon or n-type germanium one always finds that the traps dominate the recombination

at low temperatures, say below $\sim 190^{o}K$. Curtis et.al.,[9] have suggested that in neutron-irradiated n-type silicon of $\approx$10 ohm-cm the long-lived recombination center (trap) gives rise to defect localized energy level about 0.42 ev above the top of the valence band. The suggestion of the energy level position by Curtis appears to be consistent with our observations, more specifically we conclude that the energy level of the trap lies in the lower half of the forbidden gap. Trapping effects in n-type silicon irradiated by $\approx$25 Mev electrons have also been observed by van Lint[10] and his co-workers.

Transient resistivity and Hall effect voltage responses for 10 ohm-cm n-type silicon (sample SC-21) induced by 48 Mev electrons at $140^{o}K$ and at $295^{o}K$ exhibited the following features; (1) both the Hall voltage and resistivity voltage decay together with lifetimes of $\approx$1.5 μsec at $295^{o}K$ and $\approx$0.4 μsec at $140^{o}K$ after irradiation by 0.1 μsec electron beam pulses, (2) voltage saturation is observed in both Hall and resistivity transient signals and the saturation time decreases for irradiations performed at cold temperature (below $295^{o}K$) or for irradiation by shorter pulse length, (3) no long-lived decay is observed in either the Hall or resistivity voltage.

An experiment was designed to make a careful check of the resistivity pulse <u>during</u> the time the electron beam is irradiating the sample. In this experiment a one ohm-cm n-type sample of phosphorus-doped silicon was used (sample SC-28) and we observed the actual growth of excess carriers during the electron pulse and their subsequent decay. In Fig. 9 are shown the transient

resistivity voltage pulses for sample SC-28 irradiated at 122°K and at 296°K; we have also shown the corresponding electron beam pulses. Note that the electron beam current during 296°K irradiation (curve 1) is roughly 25% higher than for the 122°K irradiation (curve 2), however this difference is not important in discussing the features of the results. From the results of Fig. 9 it is quite clear that the buildup or growth of excess carriers during the time that the sample is being irradiated by the electron beam (2.5 microseconds) is independent of temperature since the build up portion of the curves are exactly the same, i.e., they fall on top of each other. The difference in the excess carrier decay time at 122°K and at 296°K is attributed to the known dependence of lifetime on temperature which is such that in the absence of trapping the lifetime decreases as the temperature at which the measurement is made is lowered.

Additional results on the growth and decay of excess carriers induced in one ohm-cm n-type silicon by electron beam pulses of varying width is shown in Fig. 10, in this case the sample temperature during irradiation was 296°K, these results are shown on the left hand side of Fig. 10. On the right-hand side of Fig. 10 are shown results obtained for one ohm-cm silicon irradiated at 122°K, in this case the results show the onset of voltage saturation (curve 1) and also the observable noise signals which appear during the beam current pulse. Also shown in Fig. 10 are the corresponding electron beam current pulses which induced the various resistivity voltage transient signals, the numbers on the curves refer to

electron beam pulse used to initiate a transient resistivity voltage of the same number on the curve. The results in Fig. 10 show that the carrier lifetime decreases with decreasing temperature which is exactly what is observed[2,11] in small injection minority carrier lifetime measurements made on silicon which does not contain trapping centers.

The dependence of radiation-induced excess carrier concentration on the total integrated electron beam flux in the pulse for one ohm-cm n-type silicon irradiated by pulses of 48 MeV electrons at 296°K and at 122°K is shown in Figs. 11 and 12 respectively. The excess carrier concentration was determined from the excess conductivity induced by the radiation, where it was assumed that only a negligible change in lattice mobility occurs during the pulse and no trapping centers are present. A simple calculation was made of the number of ion pairs produced by 50 MeV electrons from ionization loss in passing through the silicon sample. A value of 3.5 eV was used for the energy necessary to produce an ion-pair in silicon. The calculated values were in all cases within a factor of two of the measured values. Considering the very rough approximations made in the calculation we do not expect better agreement. More refined calculations[13] yield a better agreement with experiment[12].

The results given in Figs. 11 and 12 do not show a saturation of carrier concentration with ionization intensity (in units of integrated electron flux) up to excess carrier concentrations of $\sim 5 \times 10^{16}$ cm^{-3} whereas in earlier work by Wikner and Pereue[12] (40 ohm-cm, n-type silicon irradiated by $\approx$30 MeV electrons) it

was found that for $\Delta n \sim 5 \times 10^{16}$ cm^{-3} the experimental points were below a linear dependence of Δn on ionization intensity. We suggest that the results in Figs. 11 and 12 imply a linear excess carrier concentration change up to $\sim 5 \times 10^{16}$ cm^{-3}. The results of Wikner and Pereue(12) in the case of germanium (at 300°K) exhibited a linear dependence of Δn on ionization intensity up to $\sim 5 \times 10^{16}$ cm^{-3}. However our data are not accurate enough to see with any certainty the slight non-linearty noted by Wikner and Pereue(12). It is significant to point out that the linear dependence of excess carriers generated on the electron flux is basically what is predicted by theory(13).

The dependence of lifetime on injection was obtained for sample SC-28 and the results are shown in Fig. 13. The lifetime, τ_n, plotted in Fig. 13 is the time for excess carriers to decay in number from Δn to $\frac{\Delta n}{e}$ (e = 2.718). Assuming constant mobility and equal decay rates for holes and electrons Δn was obtained using the equation

$$\frac{\Delta n}{n_o} = \frac{\Delta V_\rho}{V_\rho - \Delta V_\rho} \frac{\mu_n}{\mu_n + \mu_p}$$

The increase of lifetime with injection level has been studied by Baicker(2) in both n- and p-type silicon. Baicker(2) used 1 MeV electron beam pulses to produce the excess carriers. Curtis et al,(9) have also found that the lifetime in silicon is increased as the injection level is increased, and in another publication(14) has reported that for $\frac{\Delta n}{n_o} \geqslant 10^{-3}$ the lifetime increases with injection level in germanium. Curtis has concluded that the position of the defect energy level in the forbidden energy gap of germanium has a direct influence on the injection level dependence of lifetime. If only a single recombination level is dominant then the lifetime vs.

injection level is linear, and an analysis of this condition was given by Blackmore[11]. The results in Fig. 13 exhibit a linear dependence of lifetime on injection and thereby strongly suggest that Blackmore's[11] analysis is applicable and one recombination level is probably dominant.

Conclusions and Summary

The experiments analyzed thus far yield the following conclusions regarding 1 to 100 ohm-cm silicon irradiated by 48 MeV electron pulses in the 120°K to 300°K temperature range.

1) In one ohm-cm silicon one can observe the actual buildup of excess carriers due to ionization during the time (2.5 μsec) the electron beam is irradiating the sample. After the electron beam is turned off one observes normal decay of excess electrons by recombination. The generation appears to be independent of irradiation temperature (in the 122-300°K range) if one uses electron beam pulses of approximately the same magnitude (see Fig. 9).

2) The linear dependence of carrier lifetime on injection (derived from measurements made at different electron beam fluxes) suggests that the recombination of excess electrons induced in silicon by 48 MeV electron beam pulses is governed or dominated by one defect energy level in the forbidden gap.

3) For low hole concentrations ($\approx$ 100 ohm-cm p-type silicon) the electron beam pulse produces a sufficiently large excess electron concentration to cause the material to become temporarily converted to n-type for about 200 μsec duration.

4) Additional evidence is given to the conclusion that the most significant transient radiation effects induced in silicon by pulsed electron irradiation ($\approx$50 MeV) is TRANSIENT IONIZATION, and transient atomic displacements are a negligible effect, and we observe no fast annealing effects.

5) A saturation in both Hall and conductivity voltage is observed in both n- and p-type silicon and can last up to 100 μsec. The duration of the saturation voltage decreases as the sample temperature during irradiation is lowered. For p-type silicon the saturation time decreases with accumulated electron dose, and this decrease in saturation time is a manifestation of the decrease in the carrier recombination lifetime as defects are introduced by the radiation.

6) Both the transient Hall and conductivity voltage decay together after a pulse of electrons has been delivered to the sample.

7) A long-lived decay in the resistivity voltage ($\sim$1-2 milliseconds) has been observed in 10 to 100Ω-cm n-type silicon which is due to imperfections in the crystals (including imperfections other than those produced by radiation). The appearance of this so-called trapping effect is more dominant at temperatures below 300°K and becomes more pronounced as the dose is increased.

REFERENCES

1. For a recent review of this work in device studies see IEEE Trans. Nuc. Sci., Vol. NS-12, October 1965. References to earlier work are cited in this issue. For a recent review of this work in basic property studies in materials see 7th International Conference on the Physics of Semiconductors 3, Radiation Damage in Semiconductors, Paris-Royaumont 1964 Dunod Paris (1965).

2. J. A. Baicker, Phys. Rev. 129, 1174 (1963).

3. R. H. Glaenzer and C. J. Wolf, J. Appl. Phys., 36, 2196 (1965).

4. In our experiments the electron beam spot at the sample position $\approx$ 1 inch in diameter, from the electron beam pulse shape recorded by the oscilloscope and camera associated with the faraday cup beam collector we can estimate the total number of electrons that have passed through a cm^2 of sample area.

5. M. J. Berger and S. M. Seltzer, "Tables of Energy Losses and Ranges of Electrons and Positrons", NASA SP-3012 (1964).

6. O. L. Curtis, Jr., and J. H. Crawford, Jr., Phys. Rev. 126, 1342 (1962).

7. J. E. Fischer and J. C. Corelli, Bull. Am. Phys. Soc., 10, 600 (1965) to appear in J. Appl. Phys. July (1966).

8. The trapping center concentration was measured using 50 nsec pulses of 150 kev X-rays to produce excess carriers by ionization and then noting the relative voltage magnitude of the long-lived voltage decay.

9. O. L. Curtis, Jr., R. F. Bass, and C. A. Germano "Impurity Effects in Neutron Irradiated Silicon and Germanium" Final Report Northrop Nortronics NARD 65-20R.

10. V.A.J. van Lint, et al., "Transient Radiation Effects", General Atomic Division of General Dynamics Report #GA-6248, March 22, 1965.

11. J. S. Blakemore, Phys. Rev., 110, 1301(1958).

12. E. G. Wikner and J. Pereue, Phys. Rev. 131, 1466 (1963).

13. J. Appel, Phys. Rev. 122, 1760 (1961); 125, 1815 (1962).

PROPERTIES OF SILICON SAMPLES BEFORE PULSED IRRADIATIONS WITH ≈ 48 MEV ELECTRONS

TABLE I

Sample and Code Number		Dopant	Temperature °K	Resistivity ohm-cm	Carrier Concentration cm^{-3}	Hall Mobility cm^2/volt-sec
n-type Si	PU	Phosphorus	80	52	2.6×10^{13}	4,400
SC-7			296	117	2.6×10^{13}	2,100
n-type Si	FZ	Phosphorus	295	164	1.8×10^{13}	2,140
SC-8			114	31	2.0×10^{13}	10,300
n-type Si	FZ	Phosphorus	296	7.8	8.8×10^{14}	1,800
SC-11			109	1.2	5.2×10^{14}	10,000
p-type Si	FZ	Boron	288	80	2.1×10^{14}	377
SC-14						
n-type Si	FZ	Phosphorus	296	9.2	3.4×10^{14}	2,000
SC-21			143	2.0	4.4×10^{14}	7,000
p-type Si	FZ	Boron	292	84	[illegible] 1×10^{14}	356
SC-18			148	32	1.7×10^{14}	1,160
			95	7.6	1.3×10^{14}	6,250

FZ indicates sample cut from floating zone Si; PU sample cut from pulled silicon.

TABLE I - Continued

Sample and Code Number		Dopant	Temperature °K	Resistivity ohm-cm	Carrier Concentration cm^{-3}	Hall Mobility cm^2/volt-sec
n-type Si	FZ	Phosphorus	298	101	3.1×10^{13}	2,000
SC-24			205	56.7	2.7×10^{13}	4,100
			140	24.9	3.1×10^{13}	8,190
p-type Si	FZ	Indium	298	95	1.5×10^{14}	440
SC-27			273	70	1.5×10^{14}	590
			96	7.2	1.2×10^{14}	7,221
n-type Si	FZ	Phosphorus	296	0.88	6.3×10^{15}	1,100
SC-28			122	0.62	6.3×10^{15}	4,000
p-type Si	PU	Boron	296	81	1.7×10^{14}	460
SC-31			123	10	1.4×10^{14}	4,400
n-type Si	FZ	Phosphorus	295	9.0	3.4×10^{14}	2,040
SC-22			121	1.5	4.0×10^{14}	10,000
n-type Si	FZ	Phosphorus	296	90.5	3.2×10^{13}	2,180
SC-16			123	17	3.6×10^{13}	1×10^4
n-type Si	PU	Phosphorus	295	11	Not Measured	Not Measured
SC-23					(Standard Sample)	
n-type Si	PU	Phosphorus	295	7.7	4.0×10^{14}	2,000
SC-30			142	2.0	4.7×10^{14}	6,700

FZ indicates sample cut from floating zone Si; PU sample cut from pulled silicon.

FZ indicates sample cut from floating zone Si; PU sample cut from pulled silicon.

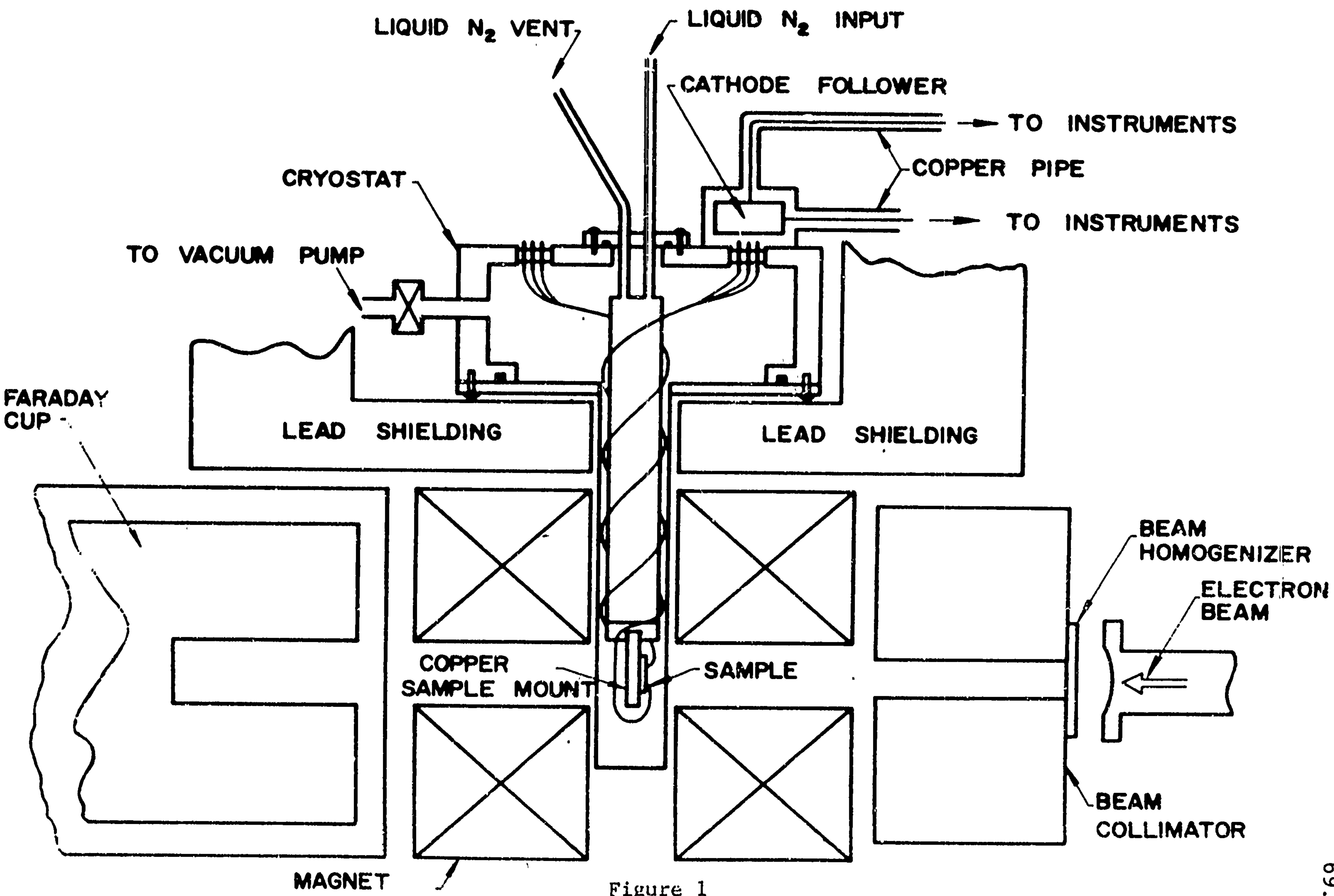

Figure 1

Schematic diagram of experimental equipment.

#23, $\frac{\Delta\rho}{\rho}$ = 95%
#24, $\frac{\Delta\rho}{\rho}$ = 94%
#26, $\frac{\Delta\rho}{\rho}$ = 66%
#27, $\frac{\Delta\rho}{\rho}$ = 27%

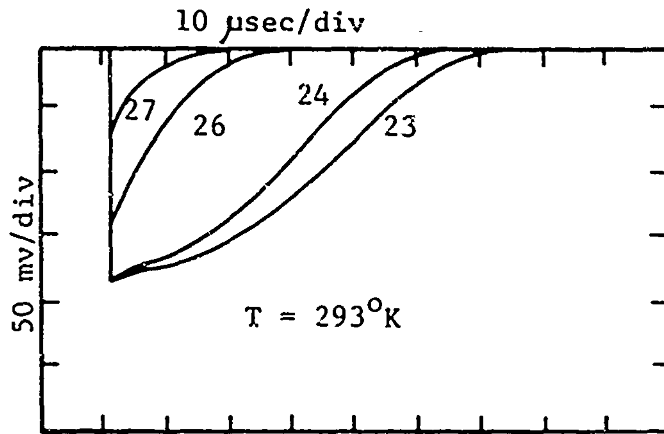

#23 $\gtrsim 3.7 \times 10^{8}$ e/cm^2
#24 $\gtrsim 2.5 \times 10^{8}$ e/cm^2
#26 $\gtrsim 3.0 \times 10^{7}$ e/cm^2
#27 LESS THAN #26

#64 $\frac{\Delta\rho}{\rho}$ = 89%
#51 $\frac{\Delta\rho}{\rho}$ = 84%
#47 $\frac{\Delta\rho}{\rho}$ = 78%
#45 $\frac{\Delta\rho}{\rho}$ = 72%
#43 $\frac{\Delta\rho}{\rho}$ = 28%

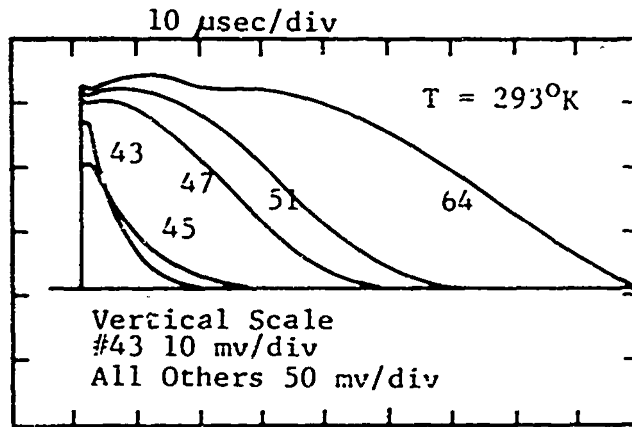

#64 $\gtrsim 1.2 \times 10^{10}$ e/cm^2
#51 $\gtrsim 3.2 \times 10^{8}$ e/cm^2
#47 $\gtrsim 1.4 \times 10^{8}$ e/cm^2
#45 $\gtrsim 7.3 \times 10^{7}$ e/cm^2
#43 LESS THAN #45

#87 $\frac{\Delta\rho}{\rho}$ = 77%
#88 $\frac{\Delta\rho}{\rho}$ = 84%
#89 $\frac{\Delta\rho}{\rho}$ = 88%
#90 $\frac{\Delta\rho}{\rho}$ = 90%
#93 $\frac{\Delta\rho}{\rho}$ = 91%
#96 $\frac{\Delta\rho}{\rho}$ = 91%

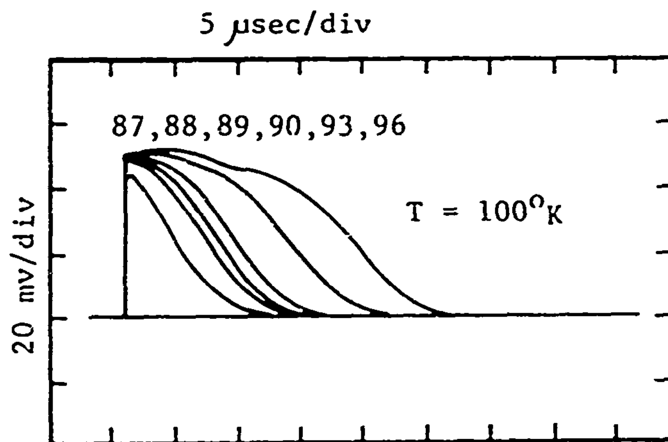

#87 $\gtrsim 1.3 \times 10^{8}$ e/cm^2
#88 $\gtrsim 3.3 \times 10^{8}$ e/cm^2
#89 $\gtrsim 5.3 \times 10^{8}$ e/cm^2
#90 $\gtrsim 1.1 \times 10^{9}$ e/cm^2
#93 $\gtrsim 4 \times 10^{9}$ e/cm^2
#96 $\gtrsim 3.3 \times 10^{10}$ e/cm^2

Figure 2
RESISTIVITY RESPONSE FOR 100Ω-cm p-TYPE SILICON (SC-27)
TO VARIED ELECTRON BEAM CURRENTS

Sample SC-18 P-Type Silicon 84 ohm-cm

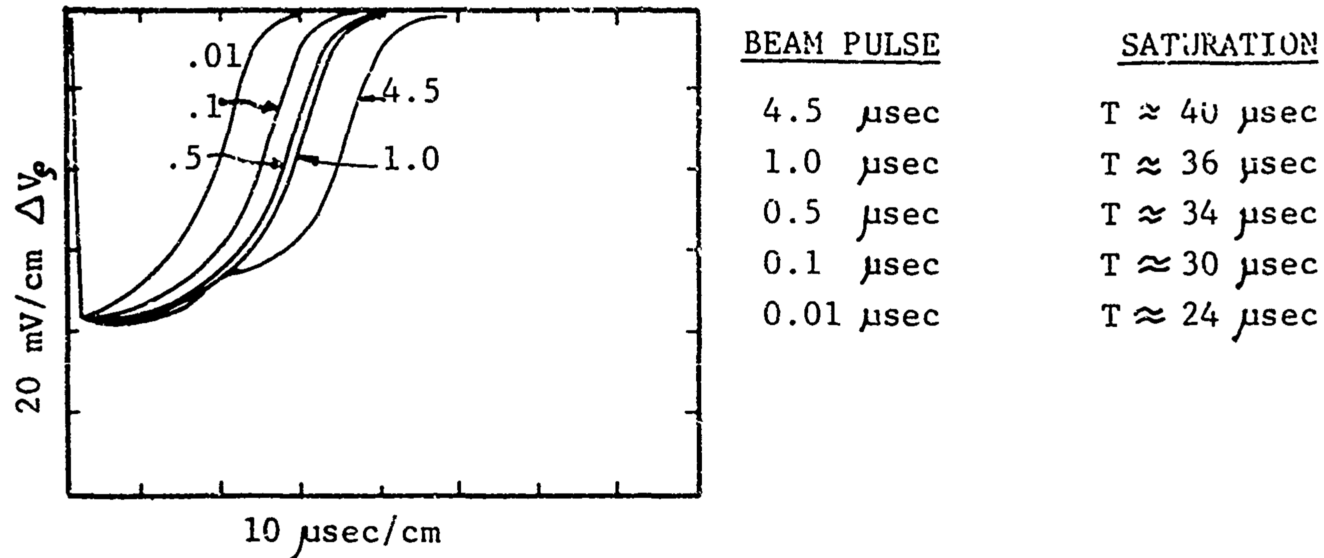

Beam Pulse	Electrons/cm^2 in Pulse	Exposure Total (Roentgens)	Exposure Rate (Roentgens/sec)
4.5 µsec	3.7×10^{11}	25,000	5.5×10^{9}
1.0 µsec	1.4×10^{11}	9,300	9.3×10^{9}
0.5 µsec	$.96 \times 10^{11}$	6,400	13×10^{9}
0.1 µsec	$.20 \times 10^{11}$	1,300	13×10^{9}

Fig. 3 Saturation time versus beam pulse width (48 MeV electrons). Also given are the electron flux and dose rate. Sample was irradiated at 295°K.

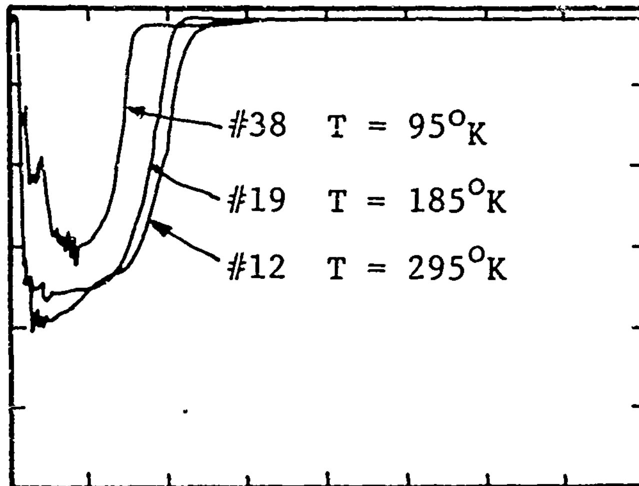

Resistivity Pulses

Sample SC-18 P-Type 84 ohm-cm

Vertical Scale #12 20 mV/cm
#19 50 mV/cm
#38 20 mV/cm

Horizontal Scale #12 20 μsec/cm
#19 20 μsec/cm
#38 5 μsec/cm

Sample I = 43 uA
I = 305 uA
I = 307 uA

Electron Beam Pulses

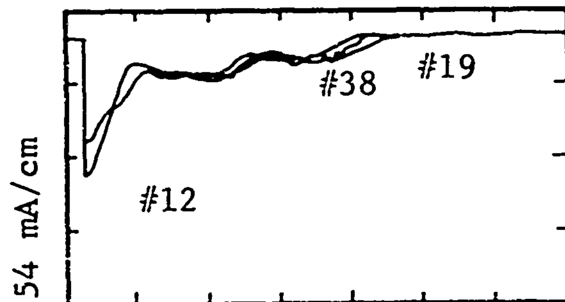

Vertical 5 V/cm thru 93 ohms
Horizontal 1 μsec/cm

These Photos Show:

1. Saturation Lifetime vs. Temp.
2. At All Temperatures $\frac{\Delta\rho}{\rho_0} \approx 95\%$

Fig. 4 Transient Resistivity Voltage Response in P-type Silicon Induced by ≈ 48 Mev Electron Pulses. Also shown are the Electron Beam pulse shapes.

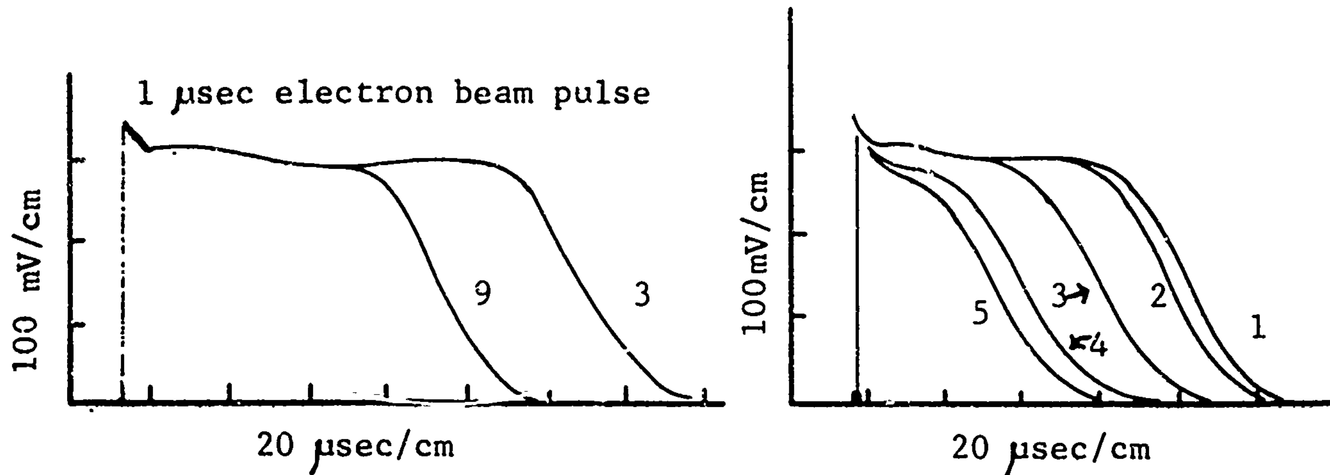

Fig. 5-a Resistivity response after 2 pulses (curve 3) and after 16 pulses (curve 9)

Fig. 5-b Resistivity response for various electron beam pulse widths

1 - 4.5 µsec
2 - 0.25 µsec
3 - 0.05 µsec
4 - 0.01 µsec
5 - 0.007 µsec

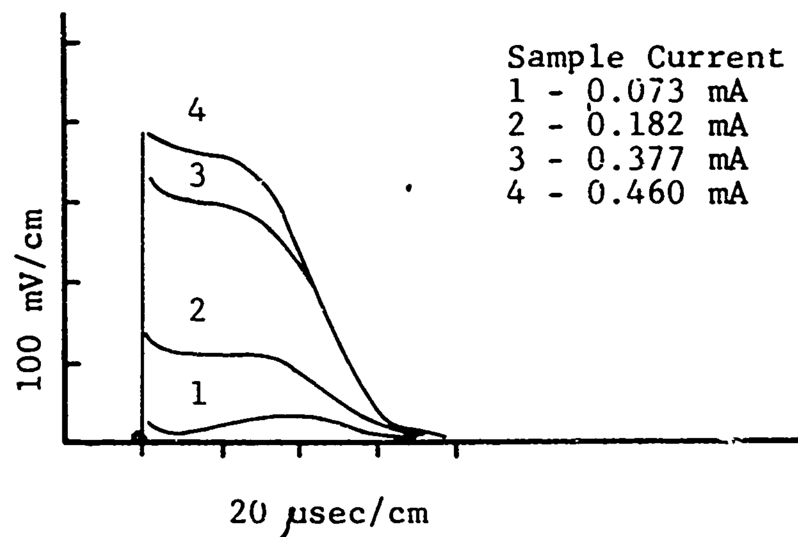

Fig. 5-c Resistivity pulses for 0.01 µsec electron beam pulse for various sample currents as shown.

Fig. 5 Response of 80 Ω-cm P-type Si (Boron Doped) to 48 MeV electron pulses at 288°K. Resistivity voltage of sample under various conditions is shown. (Sample SC-14)

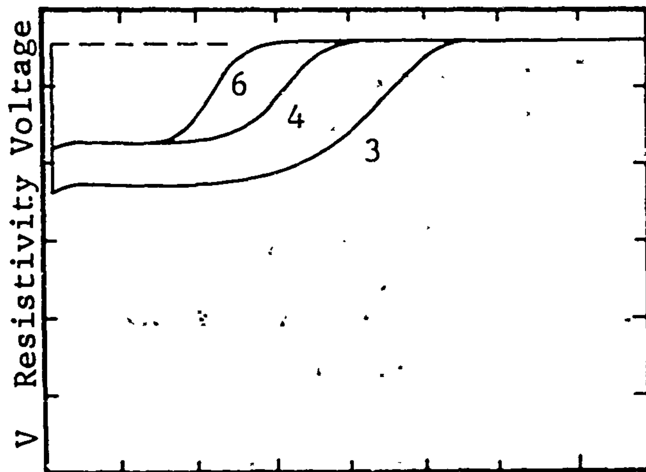

Resistivity Pulses

SAMPLE SC-18 P-type 84 ohm-cm
295°K

Vertical Scale #3 50 mV/cm
#4,6 500 mV/cm

Horzontal Scale 20 μsec/cm

Sample Current #3 59 μA
#4,6 448 μA

Photo No. Corresponds to Pulse No.

Corresponding Beam Pulse Photos

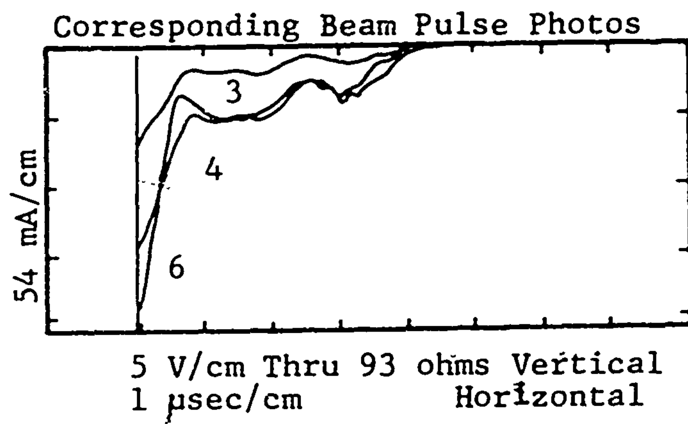

5 V/cm Thru 93 ohms Vertical
1 μsec/cm Horizontal

These Photos Show:

1. The Decay of Saturation Lifetime Due to Dose Accumulation

2. $\frac{\Delta V_\rho}{V_o} = \frac{\Delta \rho}{\rho_o}$

#4,6 $V_o = 1.30$ V $\Delta V_\rho \approx \frac{670\text{mV}}{.55} = 1.22$V

#3 $V_o = 168$ mV $\Delta V_\rho \approx \frac{90\text{mV}}{.55} = 163$ mV

(Circuit Gain ≅ 55%)

#4,6 $\frac{\Delta\rho}{\rho_o} \approx 93\%$

3 $\frac{\Delta\rho}{\rho_o} \approx 97\%$

Fig. 6 Transient Resistivity Voltage Response in p-Type Silicon Induced by ≈48 MeV Electron Pulses. Also Shown are the Electron Beam Pulse Shapes.

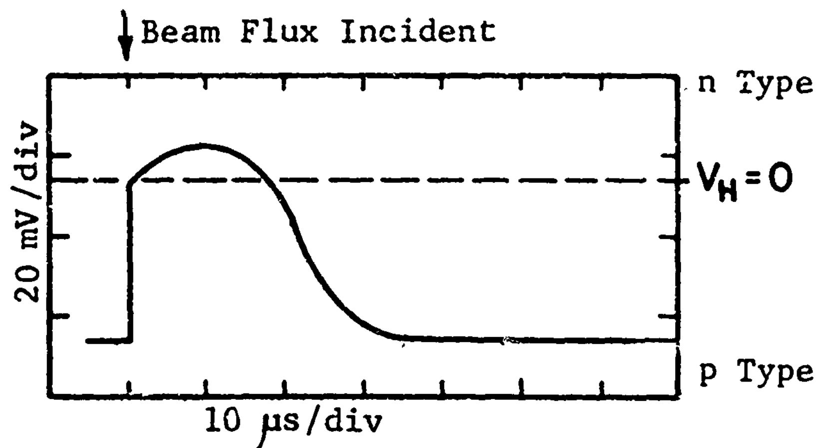

$122^{\circ}K$

Total Beam Flux
3.5×10^{8} $\frac{\text{Electrons}}{\text{cm}^2}$

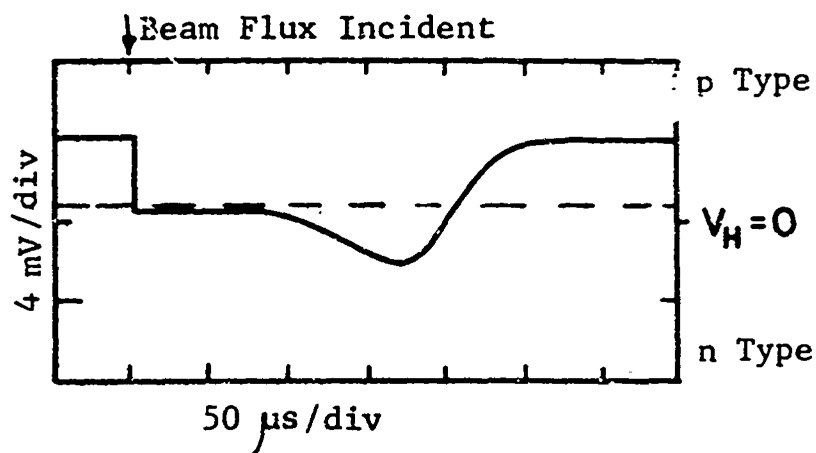

$296^{\circ}K$

Total Beam Flux
5×10^{9} $\frac{\text{Electrons}}{\text{cm}^2}$

Figure 7

Sample SC-31 100 ohm-cm p-type silicon. Hall voltage response to 48 MeV electron beam pulses at $122^{\circ}K$ and at $296^{\circ}K$. Notice that the sample appears to be n-type shortly after the irradiation. Nominal error $\pm$ 10% due to amplifier gain, parallax, scope nonlinearity. Beam pulse duration $\lesssim 1$ μs.

E = 48 MEV

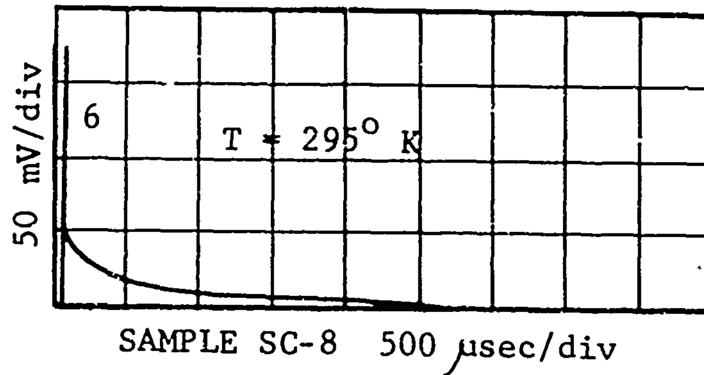

Electron Pulse Size 1 μsec
~300 ma

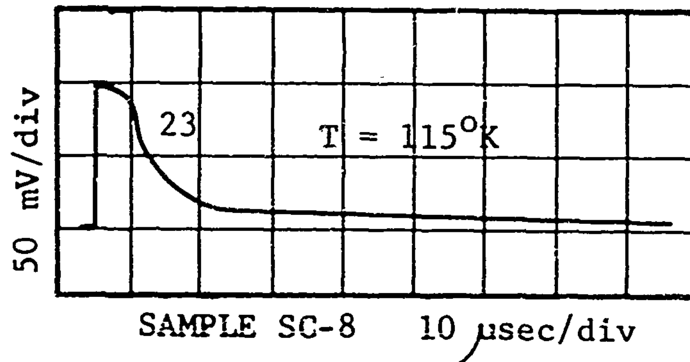

Electron Pulse Size 4.5 μsec
~400 ma

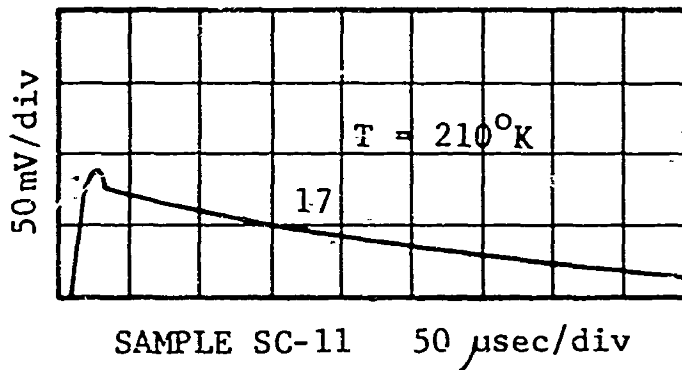

Electron Pulse Size 4.5 μsec
~150 ma

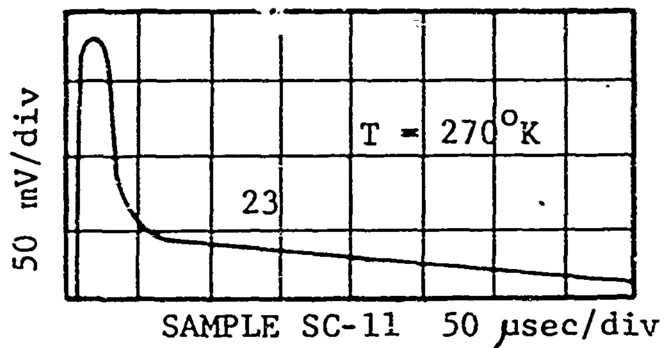

Electron Pulse Size 0.5 μsec
~500 ma

Fig. 8 Transient resistivity voltage for n-type silicon samples (see Table I).

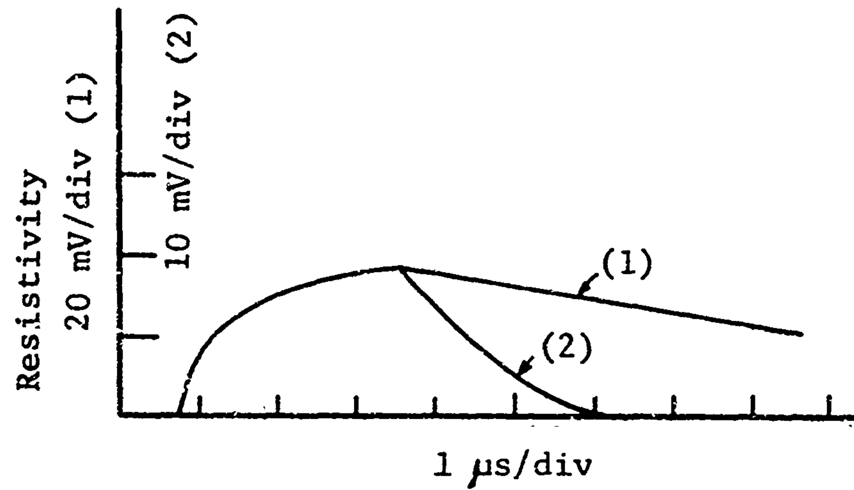

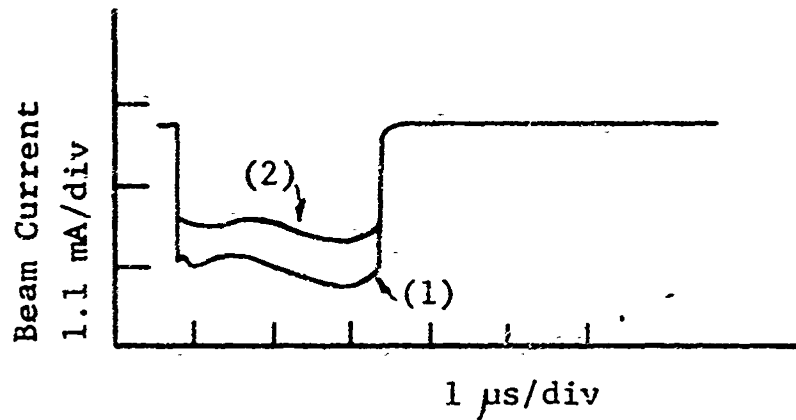

Figure 9

Growth and decay of resistivity voltage pulse in 1 ohm-cm n-type silicon (sample SC-28) irradiated at 296°K (curve 1) and at 122°K (curve 2) with 48 MeV electrons. Also shown are the corresponding electron beam pulses.

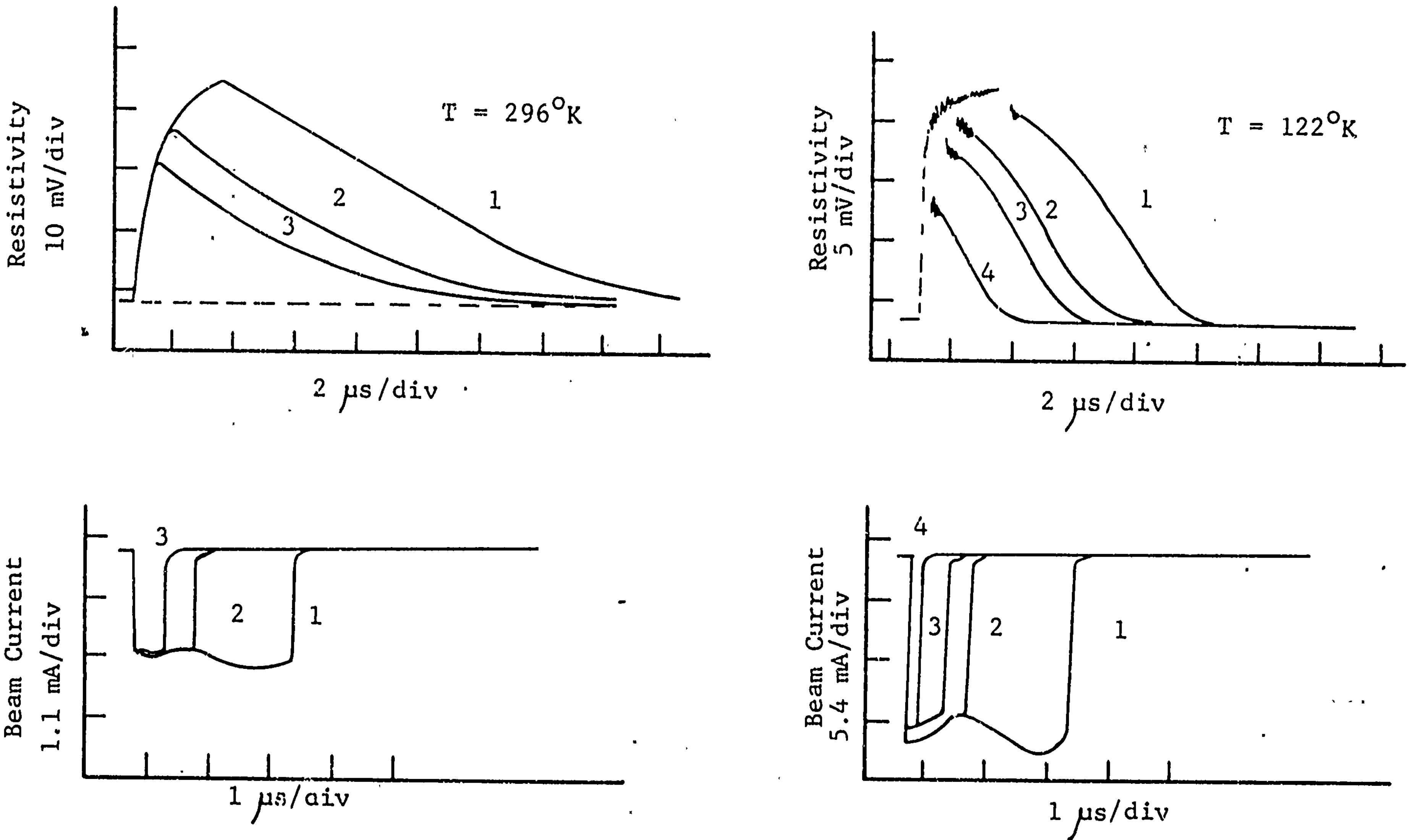

Figure 10

Response of 1 ohm-cm n-type silicon (sample SG-28) to different electron beam pulses (48 MeV). The sample was irradiated at 296°K and at 122°K.

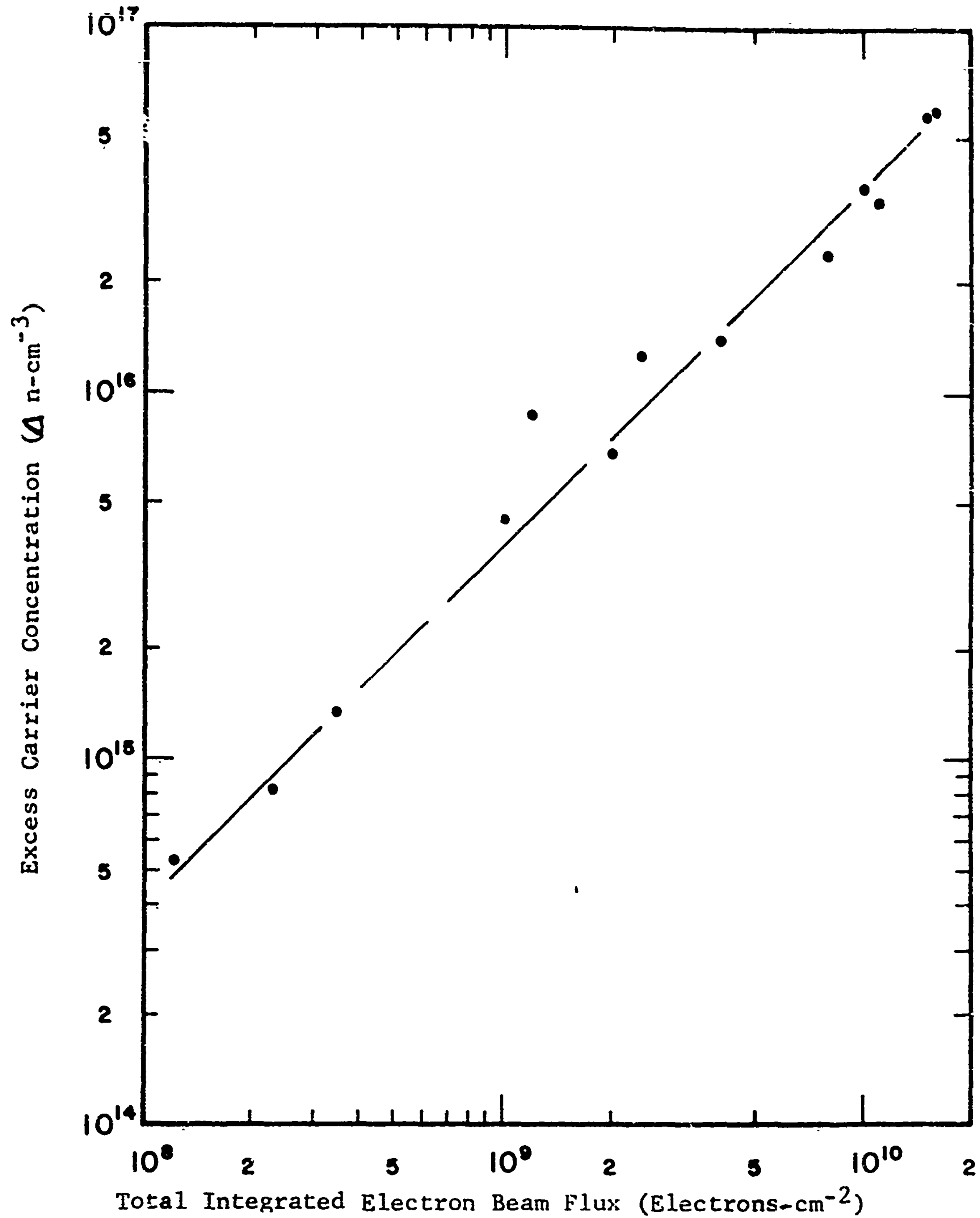

Figure 11

Sample SC-28 1 ohm-cm n-type silicon irradiated at 296°K with 48 MeV electron pulses. Nominal error is + 30% in both flux and carrier concentration.

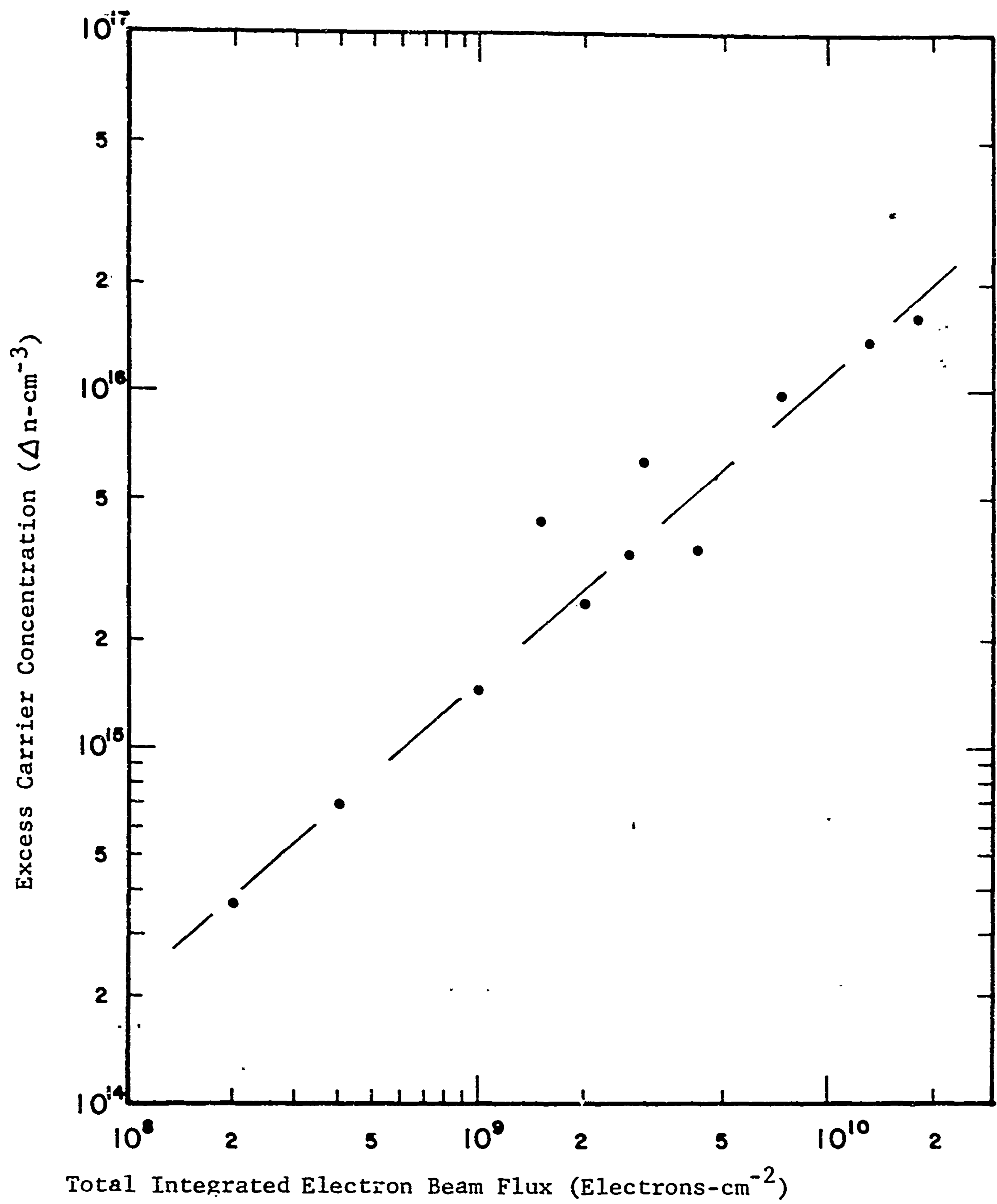

Figure 12

Sample SC-28 1 ohm-cm n-type silicon irradiated at 122°K with 48 MeV electron pulses. Nominal error is + 30% in both flux and carrier concentration.

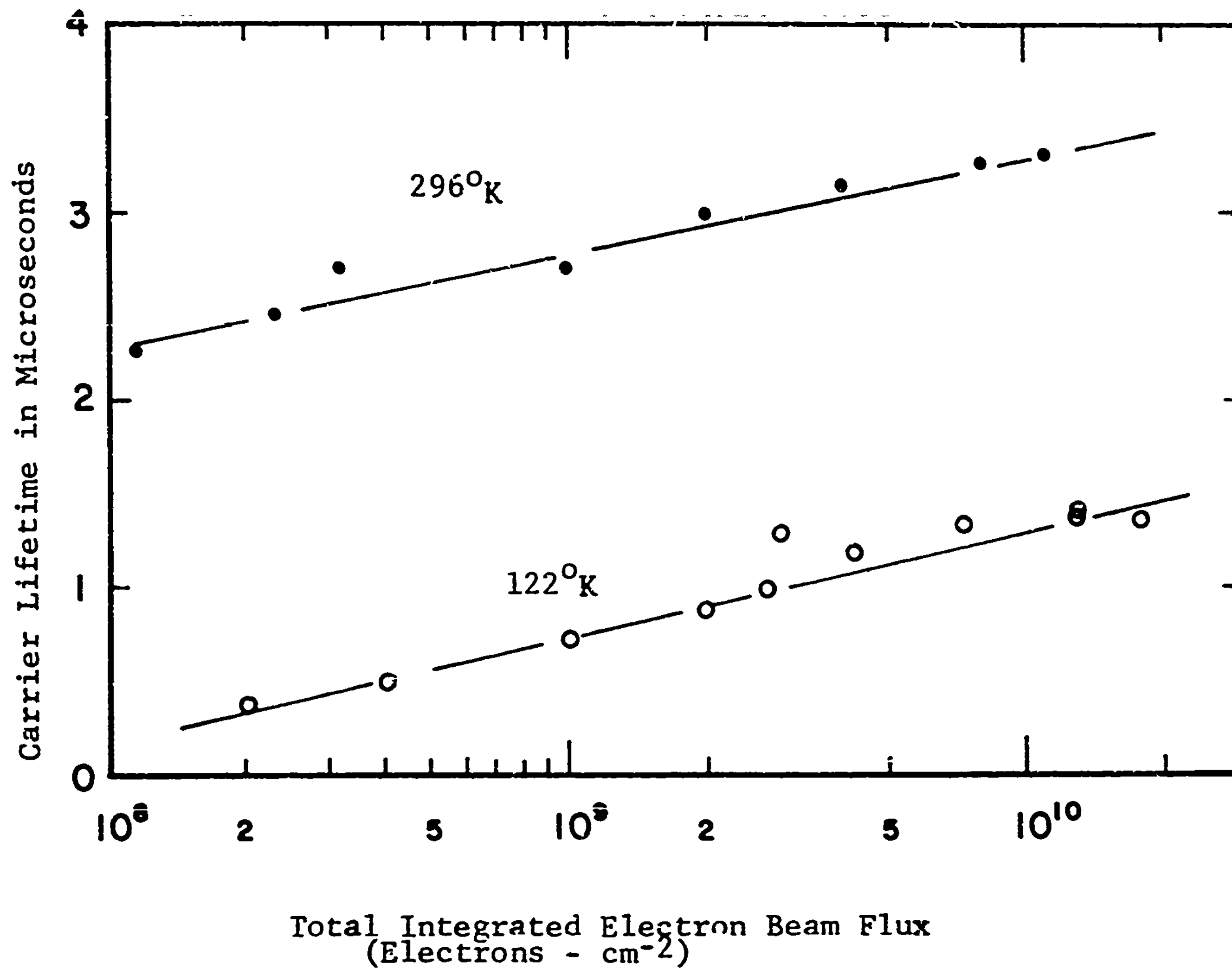

Figure 13

Sample SC-28 1 ohm-cm n-type. Lifetime vs. ionization intensity.
Notice that lifetime increases with ionization intensity.
Nominal error is ± 30% in both flux and lifetime.

Unclassified

Security Classification

DOCUMENT CONTROL DATA - R&D

(Security classification of title, body of abstract and indexing annotation must be entered when the overall report is classified)

1. ORIGINATING ACTIVITY (Corporate author) Rensselaer Polytechnic Institute, Troy, New York, 12181	2a. REPORT SECURITY CLASSIFICATION Unclassified
	2b. GROUP

3. REPORT TITLE

TRANSIENT RADIATION DAMAGE IN SEMICONDUCTOR MATERIALS

4. DESCRIPTIVE NOTES (Type of report and inclusive dates)

Final Report 1 October 1965 - 30 September 1966

5. AUTHOR(S) (Last name, first name, initial)

Corelli, John C. (Dr.)
Frederickson, Arthur R.
Westhead, James W.

6. REPORT DATE	7a. TOTAL NO. OF PAGES	7b. NO. OF REFS
December 1966	82	33

8a. CONTRACT OR GRANT NO. DA 28-043 AMC-01788(E)	9a. ORIGINATOR'S REPORT NUMBER(S)
b. ~~PROJECT NO.~~ AMC Code 5900 21 830 44 00	
c.	9b. OTHER REPORT NO(S) (Any other numbers that may be assigned this report) ECOM-01788-F
d.	

10. AVAILABILITY/LIMITATION NOTICES

Distribution of this document is unlimited.

11. SUPPLEMENTARY NOTES	12. SPONSORING MILITARY ACTIVITY
DASA Supported	U.S. Army Electronics Command, Fort Monmouth, New Jersey 07703 (AMSEL-KL-IC)

13. ABSTRACT The transient behavior of the resistivity and Hall effect voltage in 1 to 100 ohm-cm n-and p-type silicon has been studied both during and after exposing the sample to short bursts (0.01 to 4.5 μsec) of 48 MeV electrons. The buildup of excess electrons produced by ionization during the time the electron pulse is irradiating the sample appears to be dependent on the normal excess carrier decay rate. The injection levels induced by the bombarding electrons are high ($\Delta n/n > 10^{-1}$) and in most cases the excess carrier lifetimes exhibit an increase with higher injection level. The number of excess carriers generated as a function of electron beam intensity can be calculated to within a factor of 2 from a knowledge of the ionization energy loss, the energy to form an electron-ion pair, and the total integrated electron flux. The temperature dependence of induced conductivity as a function of injection is consistent with that predicted by theory. The transient Hall voltage response of 100 ohm-cm p-type silicon for high injection levels can be approximately reproduced by calculation assuming mixed hole-electron conduction and equal hole and electron decay times by a single time dependent exponential. A simple model is given which describes fast annealing in 45-50 MeV electron-irradiated silicon. The single dominant "radiation damage" process which occurs in all cases is the production of excess carriers from ionization of lattice atoms and their subsequent decay by recombination. Atomic displacement effects as manifested by the electronic transport properties appear to be very small and insignificant.

DD FORM 1 JAN 64 1473

Unclassified

Security Classification

83. Uncl

Security Classification

14. KEY WORDS	LINK A		LINK B		LINK C	
	ROLE	WT	ROLE	WT	ROLE	WT
Silicon lifetime measurement						
Resistivity (1 to 100 ohm-cm n- and p-type						
Transient ionization effects in silicon						
Conductivity (Transient)						
Hall effect voltage (Transient)						
Generation of excess carriers from ionization						
Pulsed radiation (48 MeV electrons)						
Simple model for fast annealing						

INSTRUCTIONS

1. ORIGINATING ACTIVITY: Enter the name and address of the contractor, subcontractor, grantee, Department of Defense activity or other organization *(corporate author)* issuing the report.

2a. REPORT SECURITY CLASSIFICATION: Enter the overall security classification of the report. Indicate whether "Restricted Data" is included. Marking is to be in accordance with appropriate security regulations.

2b. GROUP: Automatic downgrading is specified in DoD Directive 5200.10 and Armed Forces Industrial Manual. Enter the group number. Also, when applicable, show that optional markings have been used for Group 3 and Group 4 as authorized.

3. REPORT TITLE: Enter the complete report title in all capital letters. Titles in all cases should be unclassified. If a meaningful title cannot be selected without classification, show title classification in all capitals in parenthesis immediately following the title.

4. DESCRIPTIVE NOTES: If appropriate, enter the type of report, e.g., interim, progress, summary, annual, or final. Give the inclusive dates when a specific reporting period is covered.

5. AUTHOR(S): Enter the name(s) of author(s) as shown on or in the report. Enter last name, first name, middle initial. If military, show rank and branch of service. The name of the principal author is an absolute minimum requirement.

6. REPORT DATE: Enter the date of the report as day, month, year; or month, year. If more than one date appears on the report, use date of publication.

7a. TOTAL NUMBER OF PAGES: The total page count should follow normal pagination procedures, i.e., enter the number of pages containing information.

7b. NUMBER OF REFERENCES: Enter the total number of references cited in the report.

8a. CONTRACT OR GRANT NUMBER: If appropriate, enter the applicable number of the contract or grant under which the report was written.

8b, 8c, & 8d. PROJECT NUMBER: Enter the appropriate military department identification, such as project number, subproject number, system numbers, task number, etc.

9a. ORIGINATOR'S REPORT NUMBER(S): Enter the official report number by which the document will be identified and controlled by the originating activity. This number must be unique to this report.

9b. OTHER REPORT NUMBER(S): If the report has been assigned any other report numbers *(either by the originator or by the sponsor)*, also enter this number(s).

10. AVAILABILITY/LIMITATION NOTICES: Enter any limitations on further dissemination of the report, other than those imposed by security classification, using standard statements such as:

(1) "Qualified requesters may obtain copies of this report from DDC."

(2) "Foreign announcement and dissemination of this report by DDC is not authorized."

(3) "U. S. Government agencies may obtain copies of this report directly from DDC. Other qualified DDC users shall request through ________________."

(4) "U. S. military agencies may obtain copies of this report directly from DDC. Other qualified users shall request through ________________."

(5) "All distribution of this report is controlled. Qualified DDC users shall request through ________________."

If the report has been furnished to the Office of Technical Services, Department of Commerce, for sale to the public, indicate this fact and enter the price, if known.

11. SUPPLEMENTARY NOTES: Use for additional explanatory notes.

12. SPONSORING MILITARY ACTIVITY: Enter the name of the departmental project office or laboratory sponsoring *(paying for)* the research and development. Include address.

13. ABSTRACT: Enter an abstract giving a brief and factual summary of the document indicative of the report, even though it may also appear elsewhere in the body of the technical report. If additional space is required, a continuation sheet shall be attached.

It is highly desirable that the abstract of classified reports be unclassified. Each paragraph of the abstract shall end with an indication of the military security classification of the information in the paragraph, represented as *(TS)*, *(S)*, *(C)*, or *(U)*.

There is no limitation on the length of the abstract. However, the suggested length is from 150 to 225 words.

14. KEY WORDS: Key words are technically meaningful terms or short phrases that characterize a report and may be used as index entries for cataloging the report. Key words must be selected so that no security classification is required. Identifiers, such as equipment model designation, trade name, military project code name, geographic location, may be used as key words but will be followed by an indication of technical context. The assignment of links, rules, and weights is optional.